




# The evolution of thecideide microstructures and textures: traced from Triassic to Holocene


MARIA SIMONET RODA , ERIKA GRIESSHABER, LUCIA ANGIOLINI, DAVID A.T. HARPER, ULRICH JANSEN, MARIA ALEKSANDRA BITNER, DANIELA HENKEL, ELOY MANZANERO, TAMÁS MÜLLER, ADAM TOMAŠOVÝCH, ANTON EISENHAUER, ANDREAS ZIEGLER AND WOLFGANG W. SCHMAHL

## LETHAIA



Simonet Roda, M., Griesshaber, E., Angiolini, L., Harper, D.A.T., Jansen, U., Bitner, M.A., Henkel, D., Manzanero, E., Müller, T., Tomašových, A., Eisenhauer, A., Ziegler, A., & Schmahl, W. W. 2021: The evolution of thecideide microstructures and textures: traced from Triassic to Holocene. *Lethaia*, Vol. 54, pp. 558–577.

Thecideide brachiopods are an anomalous group of invertebrates. In this study, we discuss the evolution of thecideide brachiopods from the Triassic to the Holocene and base our results and conclusions on microstructure and texture measurements gained from electron backscatter diffraction (EBSD). In fossil and Recent thecideide shells, we observe the following mineral units: (1) nanometric to small granules; (2) acicles; (3) fibres; (4) polygonal crystals; and (5) large roundish crystals. We trace for thecideide shells the change of mineral unit characteristics such as morphology, size, orientation, arrangement and distribution pattern. Triassic thecideide shells contain extensive sections formed of fibres interspersed with large, roundish crystals. Upper Cretaceous to Pleistocene thecideide hard tissues consist of a matrix of minute to small grains reinforced by acicles and small polygonal crystals. Recent thecideide species form their shell of mineral units that show a wide range of shapes, sizes and arrangements. We find from Late Triassic to Recent a gradual decrease in mineral unit size, regularity of mineral unit morphology and orientation and the degree of calcite co-orientation. While crystallite co-orientation is the highest for fibrous microstructures, it is strikingly low for taxa that form their shell out of nanogranular to acicular mineral units. Our results indicate that Upper Jurassic species represent transitional forms between ancient taxa with fibrous shells and Recent forms that construct their shells of acicles and granules. We attribute the observed changes in microstructure and texture to be an adaptation to a different habitat and lifestyle associated with cementation to hard substrates. □ *Brachiopoda, calcite crystals, calcite fibre, EBSD, shell microstructure evolution, thecideides.*

Maria Simonet Roda  [simonet@lrz.uni-muenchen.de], Erika Griesshaber [e.griesshaber@lrz.uni-muenchen.de], and Wolfgang W. Schmahl [Wolfgang.W.Schmahl@lrz.uni-muenchen.de], Department of Earth and Environmental Sciences, LMU München, Munich 80333, Germany; Lucia Angiolini [lucia.angiolini@unimi.it], Dipartimento di Scienze della Terra "A. Desio", Università degli Studi di Milano, Milano 20133, Italy; David A.T. Harper [david.harper@durham.ac.uk], Department of Earth Sciences, Durham University, Durham DH1 3LE, UK; Ulrich Jansen [ulrich.jansen@senckenberg.de], Senckenberg Forschungsinstitut und Naturkundemuseum Frankfurt, Frankfurt am Main 60325, Germany; Maria Aleksandra Bitner [bitner@twarda.pan.pl], Institute of Paleobiology, Polish Academy of Sciences, Warsaw 00-818, Poland; Daniela Henkel [dhenkel@geomar.de], Anton Eisenhauer [aeisenhauer@geomar.de], GEOMAR-Helmholtz Centre for Ocean Research, Kiel 24148, Germany; Eloy Manzanero [manzanero.paleoart@gmail.com], Universidad Nacional de Educación a Distancia, UNED, Madrid 28040, Spain; Tamás Müller [beregond02@gmail.com], Adam Tomašových [Adam.Tomasovych@savba.sk], Earth Science Institute, Slovak Academy of Sciences, Banská Bystrica 974 01, Slovakia; Andreas Ziegler [andreas.ziegler@uni-ulm.de], Central Facility for Electron Microscopy, University of Ulm, Ulm 89081, Germany; manuscript received on 9/02/2020; manuscript accepted on 22/01/2021.

In this study, we describe and trace through time the evolution of shell microstructure and texture for a single order of rhynchonelliform brachiopods, the Thecideida. These brachiopods form a distinctive group within the Phylum Brachiopoda but obvious connections to other rhynchonelliform orders are still equivocal (Dagys 1972; Williams 1973; Frisia 1990; Carlson 2016). Thecideide brachiopods are the last brachiopod

order to appear in the fossil record (e.g. Carlson 2016). Extinct and extant thecideide species are small-bodied animals that, with the exception of very few cases (e.g. Backhaus 1959; Krawczyński, 2008), lived and live cemented to hard substrates in cryptic habitats. This lifestyle and living environment contrasts with that of most other extinct and extant Rhynchonelliformea but it is common in the Craniiformea (Williams 1973;

Baumgarten *et al.* 2013; Carlson 2016; Ye *et al.* 2018a, 2018b).

Even though the literature is replete with studies locating the Thecideida in higher taxa classifications, their position within the phylogeny of the Brachiopoda and the identification of their origin are still unclear. To shed more light on thecideide evolution, previous studies concentrated on (1) shell size and macroscale morphological features (Elliott 1953; Rudwick 1970); (2) shell structure characteristics (Williams 1973); (3) the combined interpretation of ontogenetic, morphological and shell structural properties (Baker 1990); and (4) characteristics of body size (Carlson 1995, 2007). However, even though well executed, none of these studies provided a definitive answer to either thecideide origin or to their phylogenetic relationships with other taxa, resulting most probably from their very complex and diverse evolutionary track. It is, for example, still unclear whether strophomenates, davidsonioids, spiriferides, terebratulides or other brachiopod taxa are the ancestors of the Thecideida (e.g. Pajaud 1970; Grant 1972; Williams 1973; MacKinnon 1974; Baker 1990, 2006; Lüter 2005; Cohen 2007; Carlson 2016).

The studies of Baker (2006), Williams & Carlson (2007) suggest that thecideide shell structures changed over time. This involved the following: (1) the loss of fibres; (2) restriction of fibres to small and isolated patches in the shell, for example to the cardinalia; and (3) replacement of fibres by arrangements of acicular mineral units. These changes occurred at different rates among the thecideide sub-families; fibres were suppressed by the Late Jurassic in the Lacazellinae and Thecideinae, but persisted up until the Cretaceous in the Thecidellininae (Baker 2006).

Williams and co-workers referred to the microstructure of thecideide brachiopods as a 'Primary-Acicular-Shell-Layer-Type' structure (Williams 1997), a microstructure that is developed in the outermost shell layers of all the other Rhynchonelliformea. According to Williams (1997), primary shell layer calcite is of nanometric size, has a granular morphology and contrasts significantly in dimension and morphology to other mineral units such as fibres and columns (e.g. Williams 1997; Williams & Cusack 2007). Microstructure and texture measurements carried out with high-resolution EBSD have shown that the primary shell layer of rhynchonelliform brachiopods (e.g. Goetz *et al.* 2011, and references therein) is neither nanocrystalline nor nanogranular, but consists of large (not nanogranular) interdigitating mesocrystals. These are tens of micrometre-sized dendritic calcite units that, due to their specific dendritic morphology, are interwoven in three dimensions (see Goetz *et al.* 2011, figs 4, 5). In addition, primary shell layer

mineral units of Recent rhynchonelliform brachiopods are not encased by organic material, in contrast to the mineral units in the fibrous and columnar layers (e.g. Griesshaber *et al.* 2009; Goetz *et al.* 2009; Goetz *et al.* 2011; Simonet Roda *et al.*

2019a). As illustrated in the present study, the microstructure and texture of Recent thecideide shells is distinct from that of the primary shell layer of the other rhynchonelliform brachiopods. Recent thecideides have heterogranular microstructures, where large crystals with different morphologies are embedded in a matrix of calcite nano- to microcrystallites and organic material (see also Williams 1973, 1997).

In this study, we describe the appearance and disappearance of a variety of crystal morphologies in fossil and Recent thecideide species and trace shell structure evolution from a microstructural and textural point of view. We base our results on crystal orientation measurements and not only on SEM images of fractured or etched shell surfaces (e.g. Williams 1973, 1997). By using electron backscatter diffraction imaging (EBSD), we are able to present an overview of the different types of mineral units that form the shell of the investigated thecideide species, from the Triassic to Recent, and describe the changeover from one mineral unit type to another. In addition, we reveal the different textures of the investigated thecideide species, a study that, to the knowledge of the authors, has never been attempted.

Accordingly, we present here biomineral unit type, size, morphology, orientation and their distribution pattern within the shell, degree of calcite co-orientation within as well as between mineral units for species of both thecideide superfamilies, the Thecospiroidea and the Thecideoidea; for selected specimens of taxa of the families Thecospiridae, Bactryniidae, Thecidellinidae and Thecideidae. The Thecospiridae, Bactryniidae, Thecidellinidae originated in the Late Triassic, representatives of Thecideidae have been present since the Early Jurassic. Thecospiridae and Bactryniidae became extinct in the Late Triassic and Late Jurassic, respectively, while species of the families Thecidellinidae and Thecideidae are still extant.

## Materials and methods

In this study, we show microstructure and texture results for 11 thecideide brachiopods (Table 1 and Table S1) that were chosen from a large set of samples. Each specimen represents a species and a distinct geological time interval between Late Triassic and present (Table 1 and Table S1). The investigated

Table 1. Overview of the investigated thecideide species, their age and provenance.

Families	Species	Age	Location
Thecospiridae	<i>Thecospira tenuistriata</i> (Bittner 1890)	Late Triassic	Alpe di Specie, Italy
Thecospiridae	<i>Thecospira tyrolensis</i> (Loretz 1875)	Late Triassic	Alpe di Specie, Italy
Bactryniidae	<i>Bactrynum bicarinatum</i> (Emmrich 1855)	Late Triassic	Elberg Austria
Thecideidae	<i>Neothecidella ulmensis</i> (Quenstedt 1858)	Late Jurassic (middle Oxfordian)	Baltów, Poland
Thecideidae	<i>Thecidiopsis digitata</i> (Sowerby 1823)	Late Cretaceous	Petersberg, Maastricht, Netherlands
Thecideidae	<i>Thecidea papillata</i> (Schlotheim 1813)	Late Cretaceous	Symphorien, Mons, Belgium
Thecideidae	<i>Thecidea papillata</i> (Schlotheim 1813)	Palaeocene	Ciply near Mons, Belgium
Thecideidae	<i>Lacazella mediterranea</i> (Risso 1826)	Late Eocene	Dnipropetrovsk, Ukraine
Thecideidae	<i>Lacazella mediterranea</i> (Risso 1826)	Late Oligocene	Pierre Aquitaine Basin, France
Thecidellinidae	<i>Thecidellina</i> sp.	Pleistocene	Curaçao, Caribbean
Thecideidae	<i>Pajaudina atlantica</i> (Logan 1988)	Recent	Palma, Canary Islands, Spain

specimens are housed in the collections of Ludwig Maximilian University, Munich (numbers prefixed E, LMU and UF), and Museo di Paleontologia, Dipartimento di Scienze della Terra, Università degli Studi, di Milano (numbers prefixed MPU) (see Fig. S1). For *Thecidea papillata* and *Lacazella mediterranea*, we investigated an Upper Cretaceous and Palaeocene as well as an Upper Eocene and Upper Oligocene specimen, respectively.

The shells were cut along the symmetry plane, from the umbo to the anterior shell margin. Measurements were made on cross-sections through the valves. The microstructure of both valves was investigated. The entire valve cross-section was scanned with EBSD, if possible, with one large measurement. In the case of thick valves, two EBSD scans were placed next to each other. However, care was taken that the entire cross-section of the valve, from outer to inner shell portions, from exterior to interior shell regions, is scanned with EBSD.

Special care was taken to avoid the investigation of poorly preserved shell regions. Shell surfaces that were scanned with EBSD were checked, prior to EBSD measurements, for diagenetic alteration with five screening methods: light, laser confocal, cathodoluminescence, SEM microscopy and electron dispersive spectroscopy (EDS). EDS measurements were done for the detection of Mn and Fe enrichments within the shells, as these could indicate diagenetically altered shell. EBSD measurements were carried out only on those surfaces that showed excellent preservation. With the exception of *Neothecidella ulmensis*, we performed three or four EBSD measurements on each fossil shell and 22 on the shell of the modern thecideide species *Pajaudina atlantica*. As *N. ulmensis* appears to be a transitional form between fibrous and acicular microstructures, we investigated this species in great detail and measured six large EBSD scans, of which we show here four measurements.

For all analytical techniques performed in this study, the shells were embedded in epoxy resin and sample surfaces were polished with a sequence of five mechanical grinding and polishing steps. The last step was etch-polishing with colloidal aluminium in a vibratory polisher. For the measurements, all samples were coated with 4–6 nm of carbon.

EBSD and EDS measurements and SE and BSE imaging were carried out on a Hitachi SU5000 FE-SEM, equipped with a Nordlys II EBSD detector and an Oxford Instruments 80 mm<sup>2</sup> X-Max SDD energy dispersive spectrometer. EBSD measurements were performed with a step size of 0.4–0.5 µm. Data acquisition and evaluation were achieved with the Oxford Instruments AZTec and CHANNEL 5 HKL software, respectively.

Microstructures are indicated by a grey-scaled EBSD band contrast measurement and colour-coded EBSD orientation maps, respectively. The colour code is indicated either in the figure or is stated in the relevant figure caption. Similar colours indicate similar, and distinct colours highlight different crystallite orientations, respectively. Band contrast images depict the signal strength of each measurement point. High signal strengths correspond to light grey colours and indicate strong diffraction at the crystal lattice. Faint grey or dark colours are indicative of non-diffracting substances, for example polymers, or an overlap of minute crystallites that could not be indexed automatically with the EBSD software.

The texture is presented by pole figures that give density distributions of the measured orientation data. For density distributions, we use the lowest possible setting for half width and cluster size: a half width of five and a cluster size of three degrees. The half width controls the extent of the spread of the poles over the surface of the project sphere; a cluster comprises data with the same orientation. The degree of calcite co-orientation within and between mineral units is derived from density distributions of the

measured EBSD data and is given with MUD values. The MUD (multiple of uniform (random) distribution) value is calculated using the Oxford Instruments CHANNEL 5 EBSD software. A high MUD indicates high crystal co-orientation, while low MUD values reflect a low to random degree of crystallite or/and mineral unit co-orientation. For further information, see Schwartz *et al.* (2000), Schmahl *et al.* (2004), Griesshaber *et al.* (2012) and Griesshaber *et al.* (2017). Microstructure determination is based on results measured with EBSD. Accordingly, grain morphology, size, orientation, mode of co-orientation/misorientation and degree of co-orientation/misorientation are based on measurements, diffraction measurements, and not on SEM images. The term texture relates to the varieties of crystal orientations within a material and is illustrated by pole figures. The term microstructure refers to the sum of grains, their sizes, morphologies, modes of interlinkage, co- and misorientations and is highlighted with coloured EBSD maps. Similar colours visualize similar crystal orientations, and different colours indicate differences in crystal orientation.

For AFM imaging, shell pieces were cut in longitudinal section from the umbo to the commissure and embedded in epoxy resin. Embedded sample surfaces were polished in five sequential mechanical steps down to a grain size of 1 µm. For the final step, etch-polishing was applied for three hours with a colloidal alumina suspension in a vibratory polisher. Subsequently, the samples were washed in Milli-Q water in ultrasonic bath and subsequently rinsed with 80% ethanol.

In order to expose the distribution of biopolymers and mineral units, shell pieces were glued onto aluminium rods. First, even sample surfaces were obtained by cutting and polishing the samples with glass and diamond knives in an ultramicrotome. Subsequently, sample surfaces were etched slightly, and organic material was chemically fixed. Simultaneous etching of the calcite and fixation of organic material was done by using a 0.1 M HEPES (pH = 6.5) and 2.5% glutaraldehyde solution that was applied to the sample for 180 s. Etching and fixation was followed by dehydration in 100% isopropanol three times and immediate critical point drying. The dried samples were coated for SEM imaging with 6 nm platinum.

A phylogenetic tree was constructed for the Order Thecideida. For this purpose, the software Tree-Search (Brazeau *et al.* 2019) was selected and the data matrix of Jaecks & Carlson (2001) was adopted. The latter was complemented with information on shell microstructure and texture from the taxa analysed for this study and the inclusion of *N. ulmensis* (Table

S2). For the calculations, we applied implied weighting and chose a default value of 4 for concavity, for the thecideide phylogenetic analysis.

In the text, we refer to the term ‘mineral unit’. *Mineral units* in biological structural materials are the biocrystals; in thecideide shells, biocrystals/mineral units are *fibres, acicles granules and grains*. In this study, we use terms such as *minute, small* and *large* mineral units. A *minute* mineral unit is a sub-micrometre to very few micrometre-scale entity, *small* mineral units have 2D extensions of very few micrometres, and *large* mineral units have 2D sizes of very few tens of micrometres.

## Results

Figure 1 presents the stratigraphical range and the thecideide species that were investigated in this study. EBSD results are shown in Figures 2–10, S1–S16.

We observe five different biomineral units in the investigated shells. Based on morphology and size,

Phanerozoic	Cenozoic	Quaternary	Holocene	<i>Pajaudina atlantica</i>
			Pleistocene	<i>Thecidellina</i> sp.
		Neogene	Pliocene	
			Miocene	
		Paleogene	Oligocene	<i>Lacazella mediterranea</i>
			Eocene	<i>Lacazella mediterranea</i>
	Paleocene		<i>Thecidea papillata</i> <i>Thecidea papillata</i> <i>Thecidopsis digitata</i>	
	Mesozoic	Cretaceous	Late	
			Early	
		Jurassic	Late	<i>Neothecidella ulmensis</i>
			Middle	
			Early	
		Triassic	Late	<i>Bactrynum bicarenatum</i> <i>T. tenuistriata, T. tyrolensis</i>
	Middle			
	Early			

Fig. 1. Stratigraphical distribution of the thecideide species investigated in this study. [Colour figure can be viewed at [wileyonlinelibrary.com](http://wileyonlinelibrary.com)]

we can distinguish fibrous, granular, acicular, small polygonal and large rounded biocrystals. The shell of the Upper Triassic *Bactrynum bicarinatum* Emmrich, 1855 (Figs 2A, S5) contains well-preserved stacks of fibres. Their morphology is very similar to the fibre shape that builds the secondary layer of fossil and extant rhynchonellide and terebratulide species (Griesshaber et al. 2007; Schmahl et al. 2012; Crippa et al. 2016; Ye et al. 2018a, 2018b). However, the size of the fibres differs, such that in this thecideide species (*B. bicarinatum*), the fibres are larger in cross-section relative to that observed for Recent rhynchonellide and terebratulide fibres (Figs 2, S1B, S7 cf. Ye et al. 2018a, 2018b).

We also found well-preserved stacks of fibres in the shell of the Upper Triassic thecideide brachiopod *Thecospira tenuistriata* Bittner, 1890 (Figs 2B, S1, S6, S7), depicting clearly the typical secondary layer morphology of fibres also seen in fossil and extant rhynchonellide and terebratulide brachiopod shells. However, close EBSD examination (Figs S1B, S7) reveals that *T. tenuistriata* developed fibres with two sizes: thick fibres (left- and right-hand side in Fig. S1B) and thin fibres (central portion of Fig. S1B). In perpendicular section, thick fibres, measured on their shorter axes, have a thickness of up to 8 microns, while thin fibres have average thickness of 1.8 microns. Cross-section morphologies of the large fibres are distorted, are rather polygonal and do not show a blade-shaped cross-section of the smaller fibres (Fig. S1B). In addition to fibres, we located for both Upper Triassic species (*B. bicarinatum* and *T. tenuistriata*) another biomineral unit: polygonally shaped crystals, often with roundish morphologies, in most cases large in size (shown by yellow stars in Figs 2A, 2B, S1).

Calcite crystal co-orientation/misorientation is expressed with MUD values and is given for each EBSD measurement (Figs 2–10). MUD values are multiples of uniform orientation; thus, an MUD of 1 indicates random orientation of crystallites, and an MUD of above 700 is indicative for perfect crystallite co-orientation, for example single crystals grown from solution (e.g. Greiner et al. 2018; Yin et al. 2019). For the shells of Recent terebratulide and rhynchonellide brachiopods, we obtain MUD values that are larger than 60 (Casella et al. 2018); most values scatter between 80 and 100 (Griesshaber et al. 2017). The degree of calcite co-orientation is increased for the shell of *B. bicarinatum*, MUD value of 51. In the shell of *T. tenuistriata*, the degree of crystal co-orientation is significantly lower, MUD values scatter between 22 (Fig. 2B), 14 and 18 (Fig. S1).

The shell of the Upper Jurassic thecideide brachiopod *N. ulmensis* (Quenstedt, 1858) comprises both fibres and acicles (Figs 3, S2–S4, S8). Shell layers

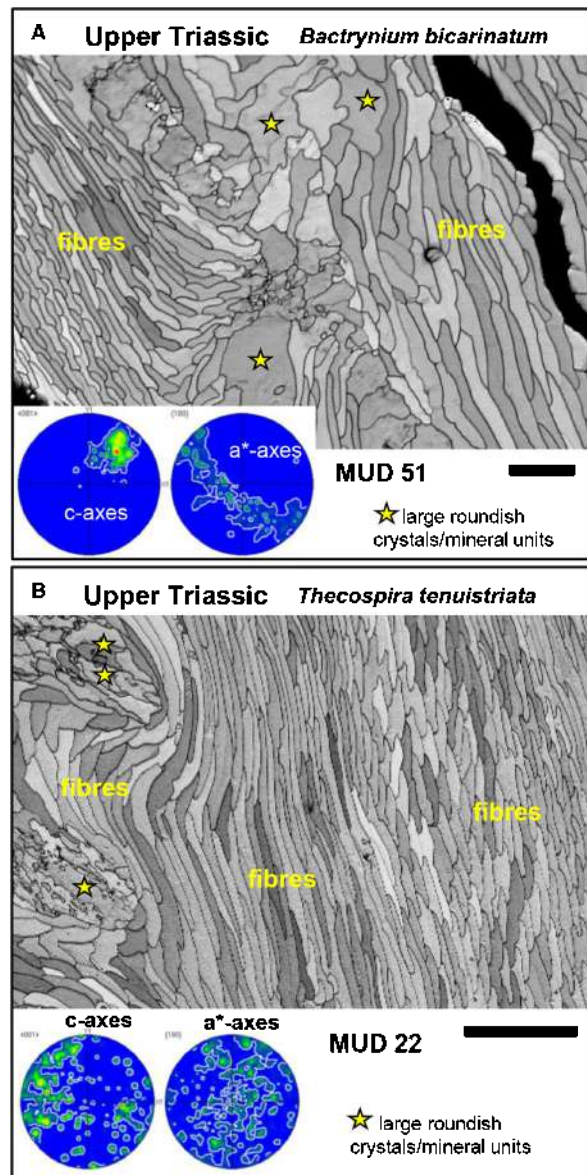


Fig. 2. EBSD band contrast images and associated pole figures depicting characteristics of the microstructure and texture of the Triassic thecideide brachiopods *Bactrynum bicarinatum* (A) (E100-18-17) and *Thecospira tenuistriata* (B) (MPU5784-4), respectively. Stacks of longitudinally and transversely cut fibres are clearly visible as well as the large roundish calcite units/biocrystals. Scale bars represent 20 and 50  $\mu\text{m}$  in A and B, respectively. [Colour figure can be viewed at [wileyonlinelibrary.com](http://wileyonlinelibrary.com)]

next to the soft tissue of the animal (innermost shell layers) consist of fibres aligned in parallel, while the outer shell is formed of acicles (Figs 3, S3, S4, S8). We conducted six large EBSD scans on shell cross-sections and observed these two microstructures in all cases; we did not detect any polygonal biocrystals. MUD values for entire scans, comprising both fibres and acicles, are increased and scatter between 30 and 40 (Fig. 3). However, if calculated individually for the different microstructures, then the degree of calcite

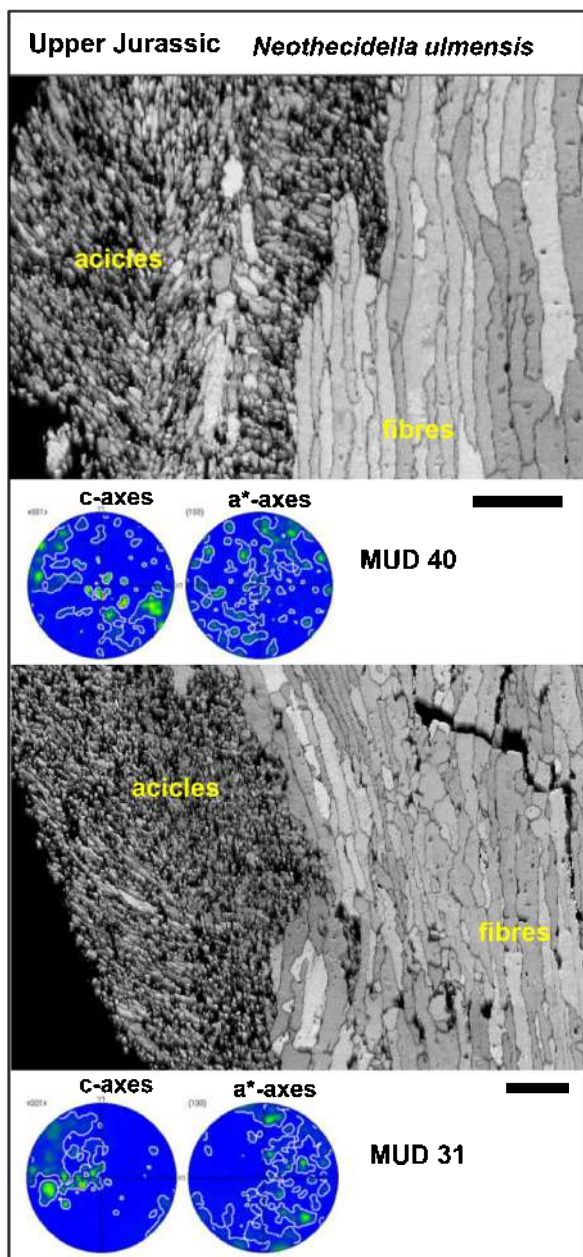


Fig. 3. EBSD band contrast images of two measurements at different shell parts and associated pole figures depicting characteristics of the microstructure and texture of the Jurassic thecideide brachiopod *Neothecidella ulmensis* (LMU-NU01). An additional measurement is given in Figure S4. Note fibrous (often with amalgamated fibres) and acicular shell portions. The stack of fibres is cut longitudinally while the acicles are cut diagonally. Scale bars represent 20  $\mu\text{m}$ . [Colour figure can be viewed at [wileyonlinelibrary.com](http://wileyonlinelibrary.com)]

co-orientation is higher for the fibres (MUD: 65, Fig. S3, MUD: 42, Fig. S4), relative to that for the acicular shell part (MUD 15/25, Fig. S3; MUD: 11, Fig. S4). Accordingly, calcite co-orientation decreases with the generation of acicular microstructures, a feature already observable for the shell of the Upper Jurassic thecideide species *N. ulmensis*.

In summary, fibres occur in all investigated Triassic and Jurassic species. In addition to fibres, Triassic taxa contain also polygonal to roundish mineral units. However, these are not developed in the shells of Upper Jurassic species. In the latter, polygonal to roundish mineral units are replaced by acicles. Calcite co-orientation is increased for the shell of Triassic *B. bicarinatum*, and it is low for Triassic *T. tenuistriata*, and is only slightly decreased relative to *B. bicarinatum*, for the Upper Jurassic *N. ulmensis*.

Acicular and granular microstructures dominate thecideide taxa from the Late Cretaceous to Holocene (Figs 4–10, S9–S16). The degree of calcite co-orientations is very low, and MUD values are below 15. For the shell of *Thecidiopsis digitata* (Sowerby, 1823), the MUD value is as low as 3.5 (Fig. 4). Acicle sizes vary and scatter between micrometre and sub-micrometre sizes (e.g. *T. papillata* (Schlotheim, 1813), Figs 5, 6); the acicles are always embedded in a matrix of nanometric to micrometre-sized granules. In addition to acicles, polygonal crystals appear (Palaeocene *T. papillata* (Schlotheim, 1813), Fig. 6; Eocene and Oligocene *L. mediterranea* (Risso, 1826), Figs 7, 8; Pleistocene *Thecidellina* sp., Fig. 9); however, these are significantly smaller in size relative to those that we found in the shell of Triassic taxa (e.g. in the shell of *B. bicarinatum* (Fig. 2A)). As stated in the methods section, all samples were carefully checked with different screening methods for possible diagenetic overprint. Accordingly, we do not consider these polygonal crystals as a result of diagenetic alteration, but rather as an original feature of the microstructure of these thecideide species (Palaeocene *T. papillata*; Eocene *L. mediterranea*; Pleistocene *Thecidellina* sp.). In contrast to Triassic and Jurassic thecideides, the shells of Cretaceous, Palaeogene and Pleistocene thecideide taxa are formed by numerous mineral units with different sizes and shapes. These are assembled following very little to almost random structural order (Figs 4–9, S9–S13) and a very low degree of calcite crystallite and mineral unit co-orientation (MUD values 3.5, 15, 10, 8). In summary, following the Late Jurassic, a marked loss of fibrous calcite occurred. If at all present in thecideide shells, fibres are limited to particular parts of the shell, for example to articular structures.

In *T. papillata* (Late Cretaceous and Palaeocene, Figs 5, 6, S10, S11) and in the Oligocene *L. mediterranea* (Figs 8, S12), we see an alternation in the orientation of stacks of more or less aligned acicles. This resembles, to some degree, the stack alternation of co-aligned fibres in Recent terebratulide and rhynchonellide brachiopod shells (Griesshaber *et al.* 2007, 2017, Ye *et al.* 2018a, 2018b; Ye *et al.* in press).

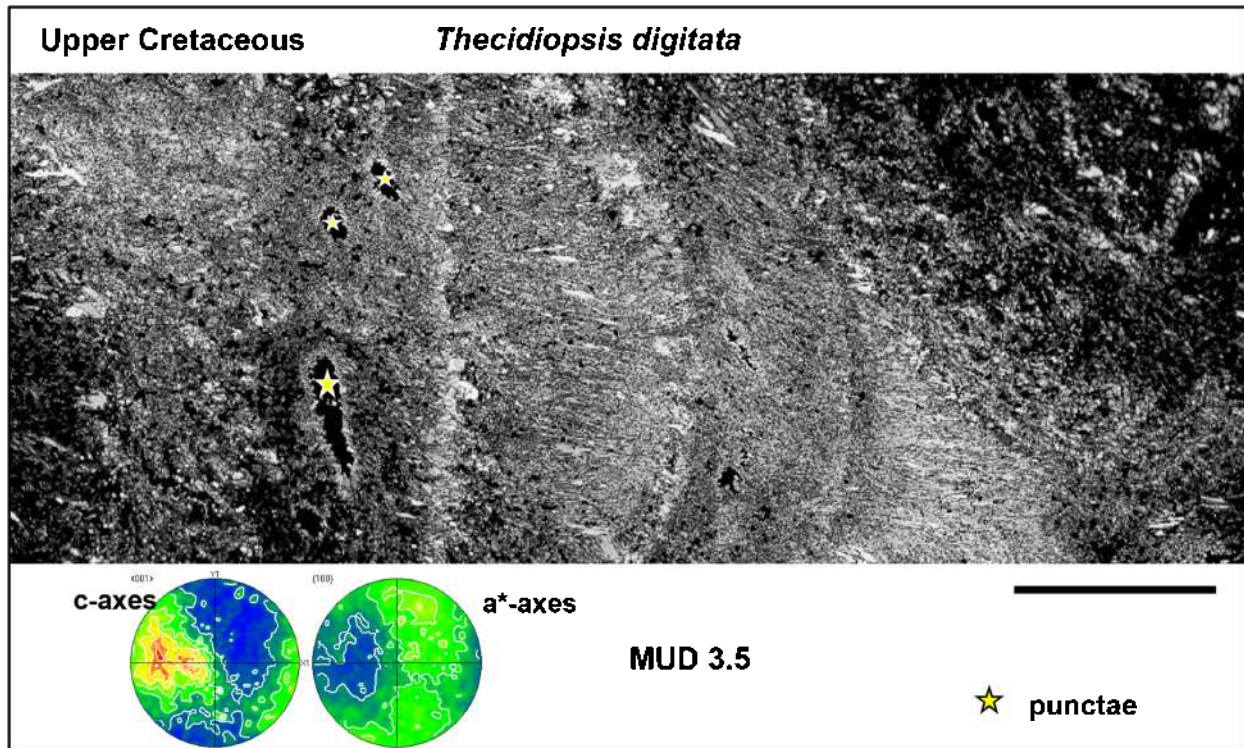


Fig. 4. EBSD band contrast image and associated pole figure visualizing the microstructure and texture of the Upper Cretaceous thecideide brachiopod *Thecidiopsis digitata* (LMU-TD01). Note the matrix of small to nanometre-sized calcite crystallites containing occluded small acicles and some small pseudo-polygonal crystals. The calcite that comprises the shell is poorly co-aligned, see the low MUD value of 3.5. Yellow stars indicate the location of punctae. Scale bar represents 20  $\mu\text{m}$ . [Colour figure can be viewed at [wileyonlinelibrary.com](http://wileyonlinelibrary.com)]

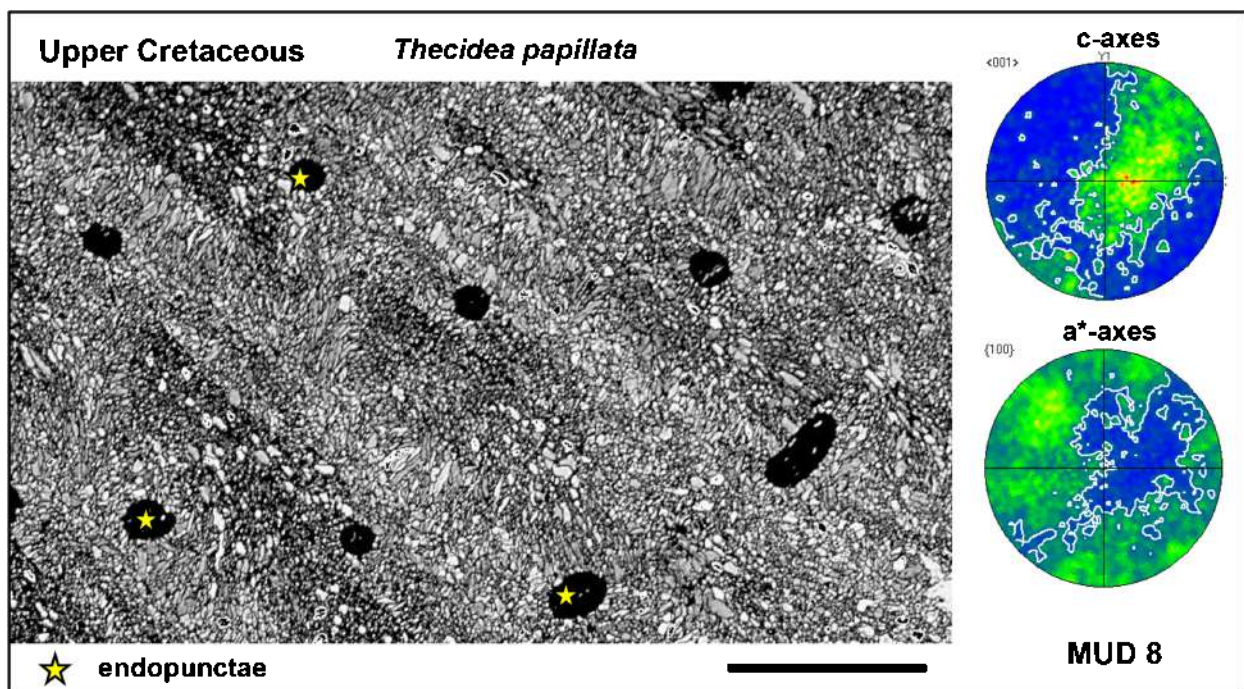


Fig. 5. EBSD band contrast image and associated pole figure visualizing the microstructure and texture of the Cretaceous thecideide brachiopod *Thecidea papillata* (LMU-TPLC01). The shell consists of acicles embedded in a matrix of small- to nanometre-sized calcite granules and small polygonal crystals. The degree of calcite co-orientation is very low (MUD value of 8). Note that endopunctae (some marked by stars) are not filled. Scale bar represents 100  $\mu\text{m}$ . [Colour figure can be viewed at [wileyonlinelibrary.com](http://wileyonlinelibrary.com)]

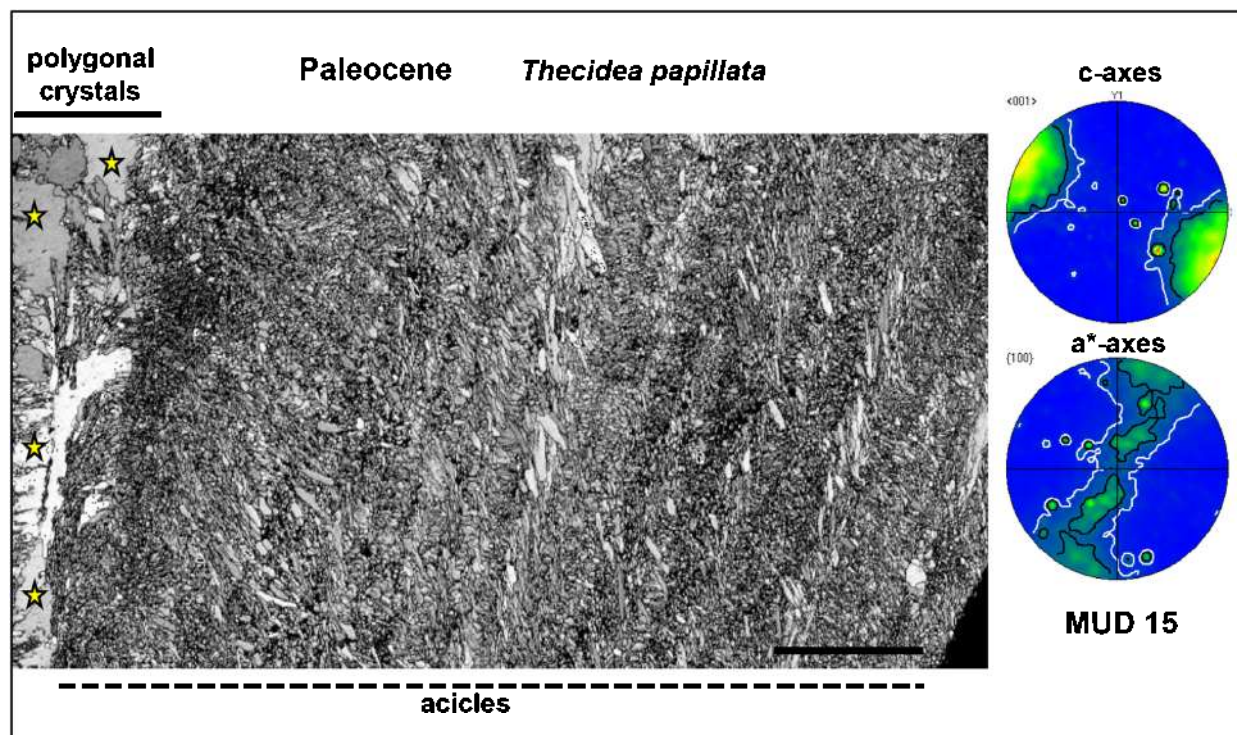


Fig. 6. EBSD band contrast image and associated pole figure visualizing the microstructure and texture of the Palaeocene thecideide brachiopod *Thecidea papillata* (LMU-TPP01). The shell consists of a matrix of nanogranules interspersed with little co-aligned acicles and some irregularly shaped, large calcite crystals (see yellow stars on the left-hand side of the image). Scale bar represents 100  $\mu\text{m}$ . [Colour figure can be viewed at [wileyonlinelibrary.com](http://wileyonlinelibrary.com)]

Figures 10, 11, S14–S16 display the microstructure and texture of the Recent thecideide brachiopod *P. atlantica*. Figure 10 presents microstructure and texture results, and Figure 11 depicts internal features of the shell such as the shapes of mineral units and the occlusion of organic membranes. We observe a large variety of mineral unit sizes and shapes: nanometre/micrometre-sized acicles, granules and polygonal crystals, all more or less randomly oriented within the shell. There is a considerable amount of organic matter intercalated into the shell of *P. atlantica*, generally developed as membranes or thin films (Fig. 11). The distribution pattern of organic matter is also unstructured, it is more or less randomly intercalated into the calcite. This is a characteristic that contrasts significantly to the distribution of organic matrices in fibrous and columnar shell layers of other Recent rhynchonelli-form brachiopods. While in the latter, organic membranes encase fibres (e.g. Simonet Roda *et al.* 2019a, 2019b) and columns, the mineral units of the primary shell layer are not sheathed by organic material (e.g. Griesshaber *et al.* 2009; Goetz *et al.* 2009; Goetz *et al.* 2011). In Recent terebratulide and rhynchonellide brachiopod shells, the primary layer consists of large, dendritic mesocrystals that interdigitate in 3D (Goetz *et al.* 2011).

Clearly visible in *P. atlantica* is the large diversity in mineral unit size and morphology (Figs 10, 11A–11C), the interlinkage of mineral units (white stars in Fig. 11B) and the presence of organic membranes/organic films that are occluded within the shell (white arrows) in Fig. 11C–11F).

## Discussion

### *Change in microstructure and texture*

The aim of this study is to trace the evolution of the thecideide microstructure and texture from the Triassic to the Recent (Figs 12–14). The change in shell fabric involves the loss of fibres and large roundish crystals/mineral units and implies the formation of acicles and granules. Thus, we see over time a change from large (micrometre-sized) biomineral units to small (sub-micrometre and nanometre-sized) biocrystals together with a reduction in microstructural order (see compilation of MUD values in Fig. 14). We observe a transition of thecideide shell fabric from co-aligned and well-assembled mineral units to almost unaligned biocrystals (Figs 12 and 14). The shells of Upper Triassic species consist of fibres and large roundish calcite crystals. The Upper Cretaceous



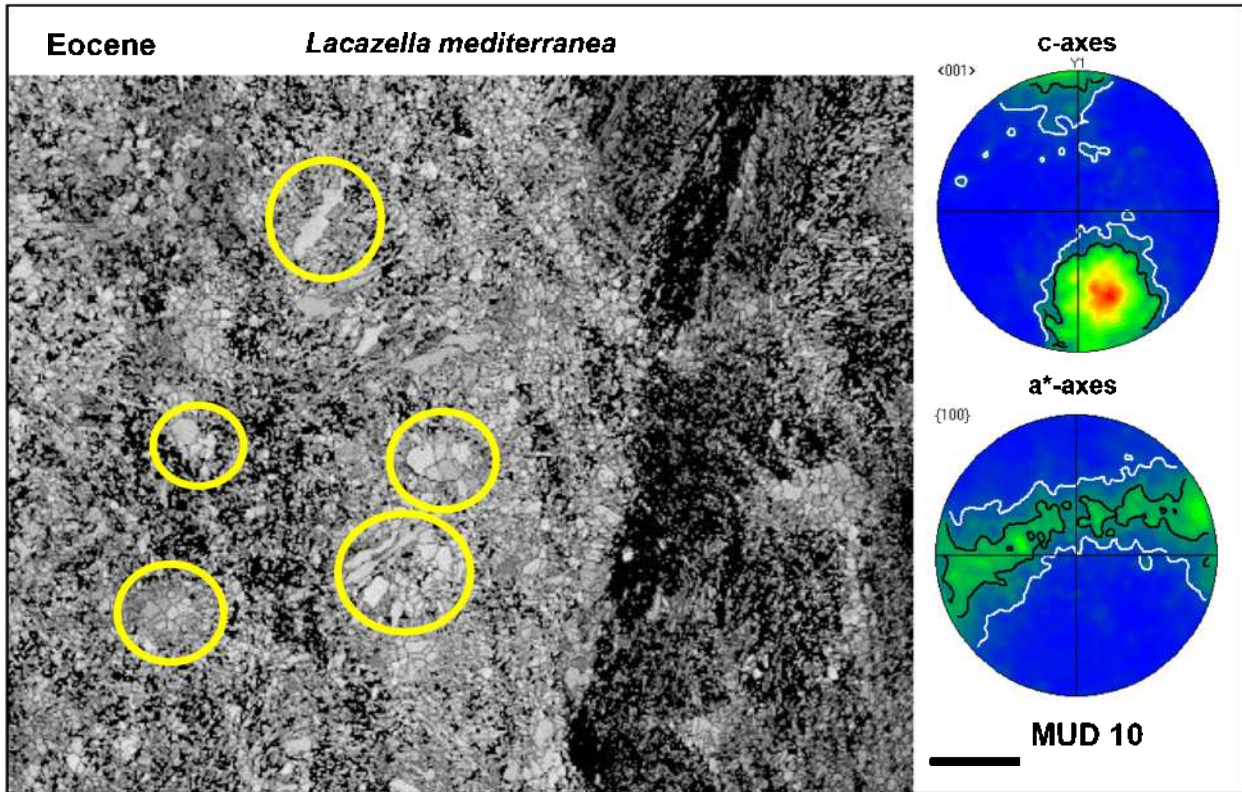


Fig. 7. EBSD band contrast images and associated pole figures depicting the microstructure and texture of the Eocene thecideide brachiopod *Lacazella mediterranea* (LMU-LME01). The microstructure of the shell is nanogranular interspersed with small polygonal calcite crystals (circled). Note very low co-orientation of calcite; MUD 10. Scale bar represents 50  $\mu\text{m}$ . [Colour figure can be viewed at [wileyonlinelibrary.com](http://wileyonlinelibrary.com)]

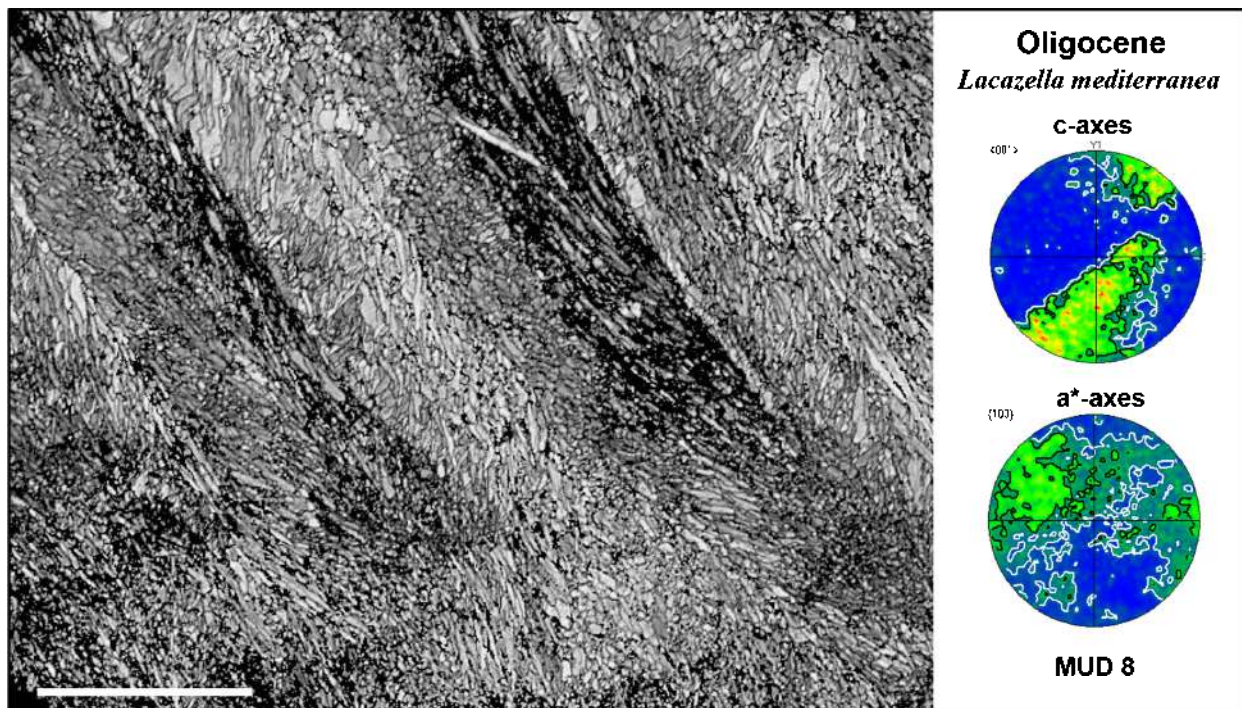


Fig. 8. EBSD band contrast images and associated pole figure depicting the microstructure and texture of the Oligocene thecideide brachiopod *Lacazella mediterranea* (LMU-LMO01). The microstructure is acicular; the acicles are poorly co-oriented. Scale bar represents 100  $\mu\text{m}$ . [Colour figure can be viewed at [wileyonlinelibrary.com](http://wileyonlinelibrary.com)]

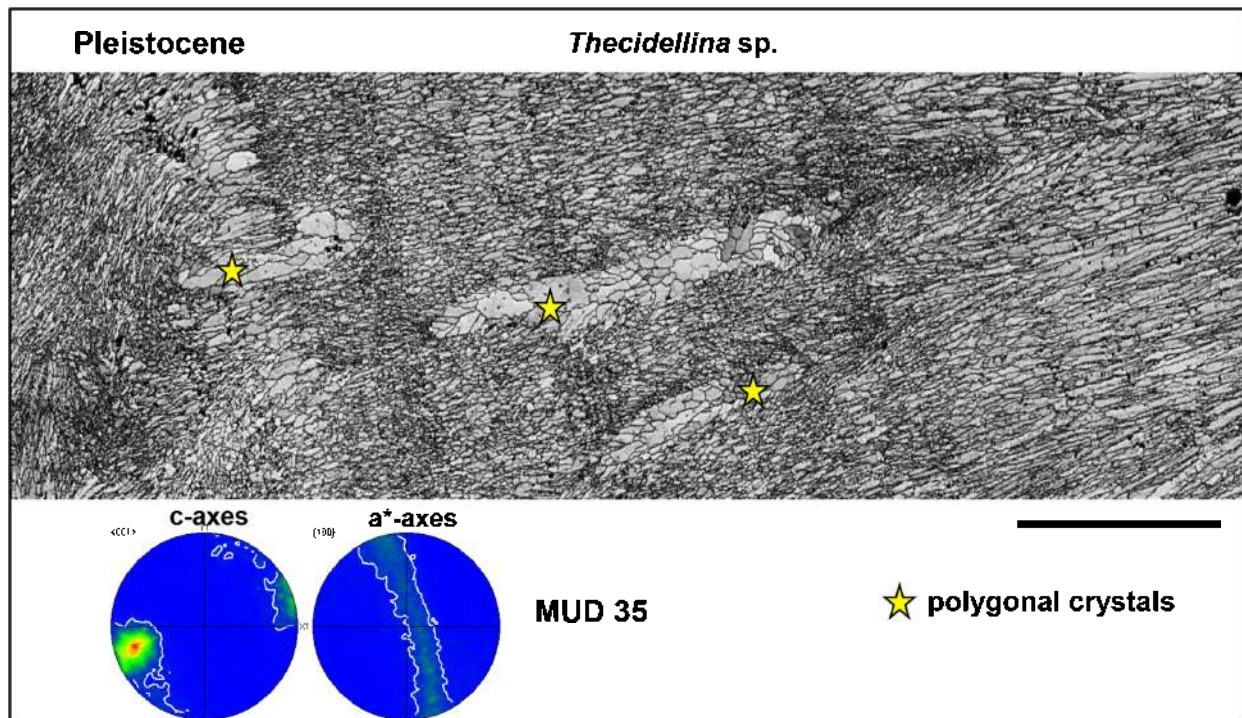


Fig. 9. EBSD band contrast image and associated pole figure depicting the microstructure and texture of the Pleistocene thecideide brachiopod *Thecidellina* sp. (UF 325201). Large stacks of acicles form the shell, interspersed with patches consisting of mainly small polygonal calcite crystals (shown by yellow stars). As the pole figure and the slightly elevated MUD value of 35 shows, co-orientation of calcite is slightly increased in the shell of this thecideide species. Scale bar represents 50  $\mu\text{m}$ . [Colour figure can be viewed at [wileyonlinelibrary.com](http://wileyonlinelibrary.com)]

to Pleistocene species built their shells of acicles, small-sized granules and small polygonal to irregularly shaped biocrystals. However, despite a significant change in microstructure, Upper Cretaceous to Pleistocene species still retain some microstructural regularity within their shells. Nevertheless, this microstructural regularity is not present in the shell of the Recent thecideide species *P. atlantica* and *Kakanuiella chathamensis* Lüter, 2005. These taxa have highly disordered, almost random shell microstructures and form their shell of a large variety of mineral units that are of highly irregular shapes and sizes (Lüter 2005). Thus, disorder in microstructure, texture and mineral unit characteristic is typical of some thecideide brachiopods, especially of those living in specific environments and having specific lifestyles. In summary, we find a decrease over time in the following: 1) biomineral shape regularity; 2) biomineral unit size; and 3) degree of biomineral unit co-orientation. All these microstructural characteristics are the least ordered in the shell of the Recent species *P. atlantica* and *Kakanuiella chathamensis*, characteristics that contrast significantly to microstructure/texture patterns of most fossil and extant rhynchonellate brachiopods. In the latter, the fibrous layer comprises well-developed stacks of co-aligned calcite fibres and, when present in the shell, the columnar layer consists of large co-aligned calcite

columns (Ye *et al.* 2018a, 2018b). In most of the Rhynchonellata, these characteristics of microstructural elements did not vary significantly from the Triassic to Recent (Ye *et al.* 2018a, 2018b).

The shell of the Upper Jurassic species *N. ulmensis* forms a special case as it consists of fibres as well as acicles and is formed exclusively of these two types of biocrystals. Both microstructures are present in the shell with a high degree of crystal co-orientation, especially the calcite of the fibrous shell layer (MUDs of 42 and 65). Crystal co-orientation within the acicular shell portion of *N. ulmensis* is increased, MUD values are 25, 15 and 11, but are not as high as in the fibrous shell layer. This finding does not support the inference of Jaacks & Carlson (2001) that the acicular microstructure is complementary to the fibres. Those taxa that have an acicular microstructure have a reduced fibrous layer, for example *N. ulmensis*. The Upper Jurassic *N. ulmensis* could be a possible link between those thecideides that fabricated their shells with fibres and large roundish crystals and those that formed their shells from small acicles and granules. In addition, *N. ulmensis* illustrates that up to Late Jurassic, thecideides were able to secrete fibres, a capability that was lost in the Early Cretaceous (this study and Baker 2006). Indeed, the Lower Cretaceous *Neothecidella parviserrata* is described as having fibres limited to teeth or to tooth ridges. Fibres in the

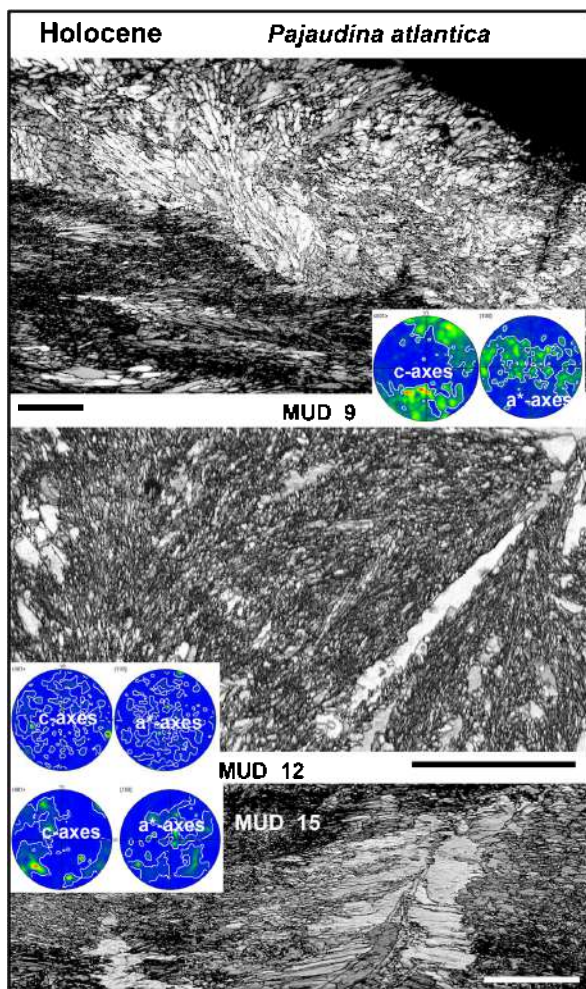


Fig. 10. EBSD band contrast image and associated pole figure depicting the microstructure and texture of the Recent thecideide brachiopod *Pajaudina atlantica* (LMU-PA008, LMU-PA0010 and LMU-PA009 from top to bottom, respectively) The shell of this brachiopod species includes all types of biocrystals: nanogranules, granules, acicles, small polygonal crystals and large polygonal crystals. The degree of calcite co-orientation is low. Scale bars represent 20  $\mu\text{m}$  for A and 50  $\mu\text{m}$  for B and C. [Colour figure can be viewed at [wileyonlinelibrary.com](http://wileyonlinelibrary.com)]

dorsal valve of *Neothecidella parviserrata* are completely suppressed (Baker & Laurie 1978). The *Neothecidella* lineage appears to confirm the suggestion of Williams (1973) that fibres might become suppressed around the Jurassic–Cretaceous boundary.

The shell microstructure of Recent thecideides was previously described as having a structure/microstructure similar to that of the primary layer of other rhynchonelliform taxa (Baker 2006; Williams & Cusack 2007). The present study indicates that this is not the case. EBSD measurements indicate that the microstructure and texture of the primary shell layer of most Recent rhynchonelliform brachiopods is an assemblage of interdigitating dendrites, micrometre-

sized calcite mesocrystals (Goetz *et al.* 2011; Schmahl *et al.* 2012; Ye *et al.* 2018a, 2018b). Dendritic mineral unit arrangements are easily detected with EBSD, even in 2D (Goetz *et al.* 2011; Griesshaber *et al.* 2017), and are distinct from microstructures that are formed by any kind of stacked mineral unit assemblages. Furthermore, neither SEM nor TEM observations were able to detect any organic components within or surrounding the mineral units of the primary layer (e.g. Griesshaber *et al.* 2009). These features contrast to structural characteristics of Recent thecideide shells, for example that of *P. atlantica* or of *Kakanuiella chathamensis* (unpublished data and Goetz *et al.* 2009), where we do not find any dendritic mesocrystals, nor organic sheaths encasing the mineral units. However, we find organic membranes intercalated within Recent thecideide shells (Fig. 11).

Even though the shell fabric of Recent thecideides differs significantly from the other extant Rhynchonelliformea, the occurrence of fibrous layers in Upper Triassic to Cretaceous species, the presence of endopunctae with perforated canopies in several genera and the capacity to resorb shell (Baker 2006 and reference therein) make the thecideide shell fabric more similar to that of the Rhynchonellata and less akin to Strophomenata shell microstructures, although the latter have also a complex shell fabric, that consists of laminae of aligned blades (Garbelli *et al.* 2014; Ye *et al.* in press). Accordingly, as outlined above, we wish to emphasize with this study that, on the basis of shell fabric and microstructure, it is very difficult to envisage a link between thecideides and strophomenates, as was previously suggested by Williams (1973), Baker (2006) and Carlson (2016).

An important feature of thecideide and terebratulide brachiopod shells is the occurrence of endopunctae. In longitudinal sections, these are canal-like structures that cross the shell in terebratulides from the innermost fibrous to the primary shell layer (Williams 1997). In thecideides, endopunctae are often suppressed (Baker & Laurie 1978); however, if present, they cross the heterogranular microstructure from innermost to outermost shell regions. In the studied samples, we see endopunctae only in the shells of the Cretaceous *T. digitata* and *T. papillata* (Figs 4 and 5). In living rhynchonelliform brachiopods, the walls and the basal region of endopunctae are covered by living cells (Williams 1997; Simonet Roda *et al.* 2019a; fig. 11). With the degradation of organic material, endopunctae could become filled with diagenetic calcite, and this might lead to misinterpretation and be seen as brachiopod shell calcite with specific crystal morphologies, sizes and orientation. In this study, we investigated the

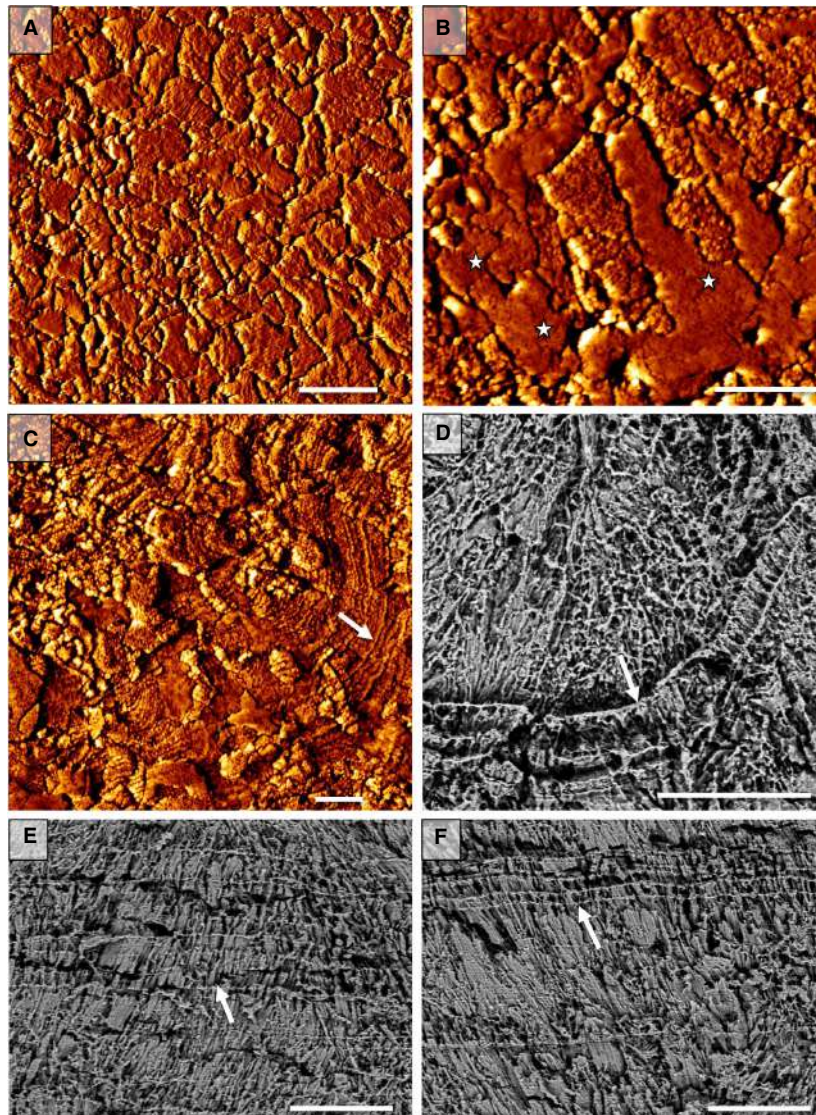


Fig. 11. Internal structural characteristics of the shell of the Recent thecideide brachiopod *Pajaudina atlantica*. A–C, AFM images (LMU-PA010); D–E, SEM images of polished and etched surfaces (LMU-PA011). The organic material is chemically fixed. The presence of organic membranes/organic films occluded within the shell is indicated with white arrows. The white stars (1B) point to the interlinkage of the mineral units. Scale bars: A–C, 2.5  $\mu\text{m}$ ; D–F 10  $\mu\text{m}$ . [Colour figure can be viewed at [wileyonlinelibrary.com](http://wileyonlinelibrary.com)]

shell material with great care for any diagenetic overprint and therefore avoided the misinterpretation of secondary calcite within endopunctae. In addition, based on structural patterns and MUD values, EBSD measurements and the analysis of orientation data provide reliable indications for the identification of diagenetic calcite within shell material (Casella *et al.* 2018), which was not observed here.

#### Phylogenetic implications

We present with this study a new phylogenetic hypothesis for the evolution of the thecideides (Fig. 13). This is not the main purpose of the paper,

however, as it provides a template to map and interpret changes in shell fabric through time against the evolution of the group. For the construction of the tree, the data matrix of Jaecks & Carlson (2001) was modified with the addition of information on the shell microstructure from the taxa analysed here and the inclusion of *N. ulmensis* (Table S2). The tree was constructed by TreeSearch (Brazeau *et al.* 2019) using implied weighting, and the default value of 4 for concavity was used and a number of characters in the terebratulide outgroup that were coded as inapplicable. The search produced a single, unique tree (Fig. 13). As already illustrated in previous phylogenetic reconstructions (e.g. Jaecks & Carlson 2001;

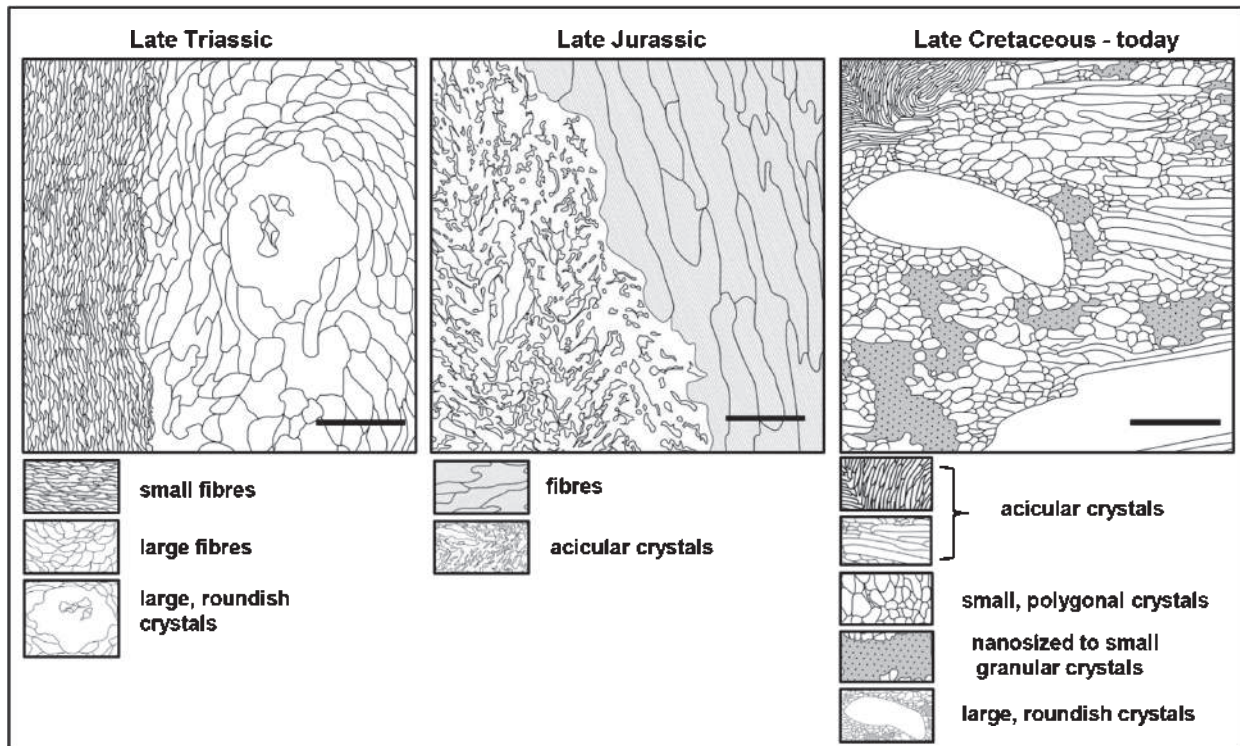


Fig. 12. Microstructure features of thecideide brachiopods characteristic for different geological intervals. Scale bars represent: 50  $\mu\text{m}$  for the Late Triassic example, 20  $\mu\text{m}$  for the Late Jurassic example and 40  $\mu\text{m}$  for the Late Cretaceous – Recent example.

fig. 5), aspects of this tree shows that there are anomalies with the current familial taxonomy of the thecideides.

Using the terebratulides as an outgroup, the basal taxon is *Thecidella* and not *Eudesella* as was the case in the original analysis of Jaecks & Carlson (2001). *Eudesella* is still, nevertheless nearby, in the lower part of the tree. This hypothesised phylogeny indicates that the Hungarithecidae and Thecospirellidae are ancestral to both Thecidellinidae and Thecideidae. There is no evidence, however, that the Hungarithecidae are ancestral to Thecidellinidae, and the Thecospirellidae are ancestral to Lacazellinae, as suggested by Baker & Logan (2011) on morphological evidence. However, in the upper part of the tree, the thecospirellid *Bittnerella* is linked to most taxa of the Lacazellinae. The same relationships were noted on their phylogenetic tree by Jaecks & Carlson (2001, fig. 5), with *Thecospirella* in the lower part of the tree and *Bittnerella* in the upper. Jaecks & Carlson (2001, p. 214) emphasized that '*Bittnerella*, one of the Triassic taxa, is consistently located near the base of the *Lacazella* clade'. *Pamirotheca* is also anomalous; in all analyses, it occurs in the mid-part of the tree.

Jaecks & Carlson (2001) demonstrated that the reduction or loss of the fibrous microstructure in most of the Thecideidae is a derived feature. Taxa

near the root of the tree have a continuous inner fibrous layer, whereas most derived taxa have fibrous layers that are reduced or absent, with the exception of *N. ulmensis* which maintains a continuous fibrous layer, as confirmed by our microstructural analysis. Another exception is the Upper Cretaceous *Eolacazella longirostrea*, which is rather low in the tree, but has a completely suppressed fibrous layer.

The pattern is more complex in the Thecidellinidae, as *Stentorina*, near the root of the tree, has a continuous fibrous layer. However, *Rioutlina* and *Eothecidellina* are more derived and have a continuous fibrous lining. Accordingly, the reduction or loss of the fibrous layer probably occurred more than twice. This analysis does not support the suggestion of Baker & Logan (2011) that Thecidellinidae emerged as a sister group to the Thecideidae in the Late Triassic, as *Thecidella* appears as a basal taxon, but the position of *Moorellina*, may be in agreement with the suggestion of Baker & Logan (2011).

The revised phylogeny confirms a number of anomalies already highlighted by Jaecks & Carlson (2001). These anomalies suggest that (1) there may be issues with the currently accepted classification of the group; (2) characters and their coding may require re-evaluation; and (3) further studies of the shell fabrics of all the thecideide taxa like those

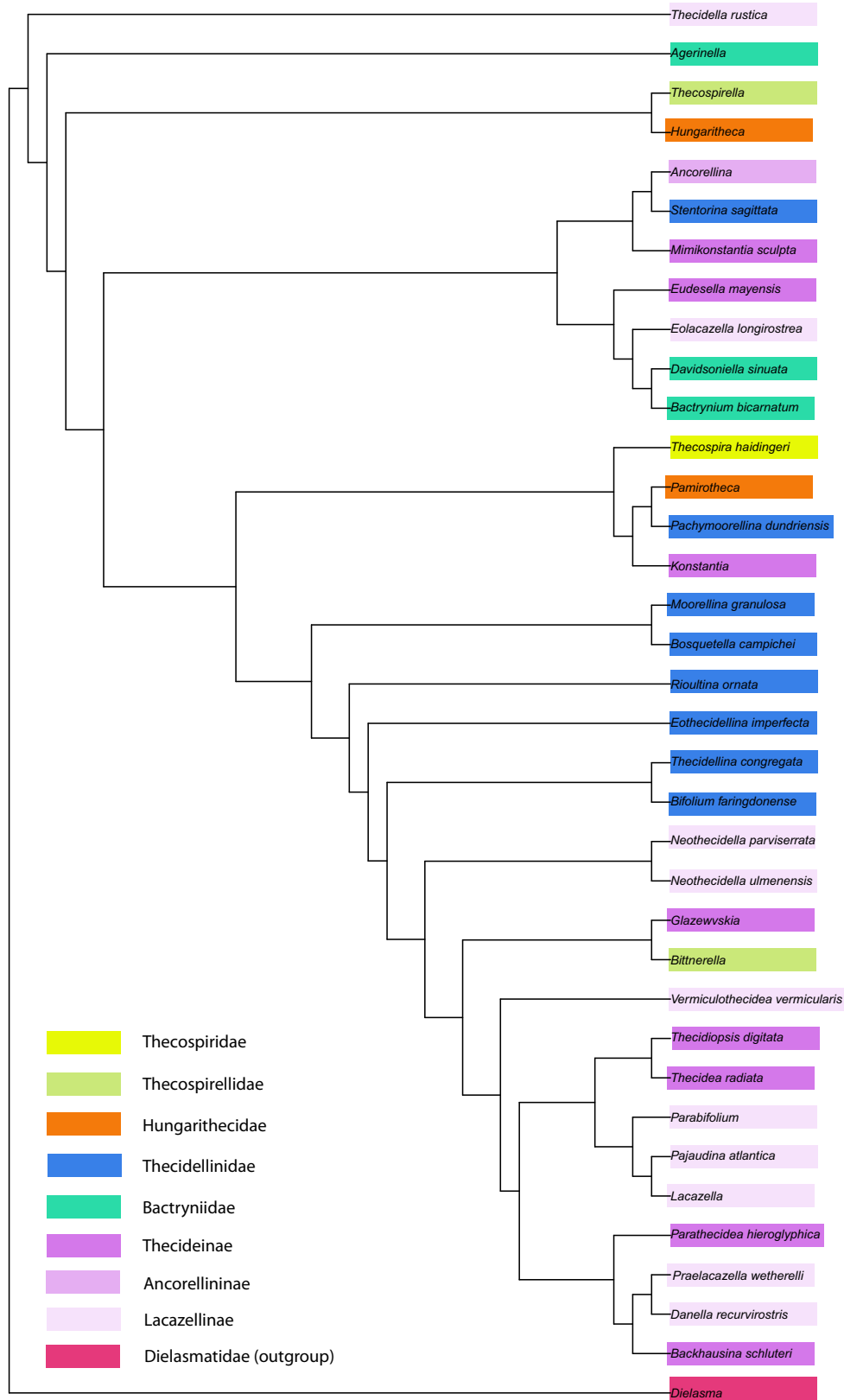


Fig. 13. Phylogenetic tree based on the characters and character states given by Jaecks & Carlson (2001) with the addition of microstructure and texture results obtained in this study and the inclusion of the thecideide species *Neothecidella ulmenensis*; the families recognized by Baker (2006) are indicated. The subfamilies Thecideinae, Ancorellininae and Lacazellinae belong to the Family Thecideidae. The tree was constructed using TreeSearch (Brazeau *et al.* 2019), details are given in the text. [Colour figure can be viewed at [wileyonlinelibrary.com](http://wileyonlinelibrary.com)]

provided in this study are required to understand the development of this important suite of characters across the group and their phylogenetic significance. Besides the appearance of acicular microstructure and the reduction/loss of the fibres, which according to Jaecks & Carlson (2001) are derived features, the different types of granular microstructures, the large roundish as well as the small polygonal crystals and the MUD values described here, should be investigated further, especially in early stocks. This is the first study that links microstructure and texture results gained from EBSD measurements and data evaluation to phylogenetic analysis and their implications.

*Is the change in microstructure an expression of adaptation to a different lifestyle and living environment?*

Brachiopods dominated global marine benthic habitats until the end of the Permian, when the largest mass extinction of marine biota in the Earth's geological history severely affected the phylum. About 90% of the species went extinct and brachiopod evolution was completely reset (e.g. He et al. 2019). However, even though the causes that led to this biotic crisis are still debated, a main feature of the End-Permian

event was the massive extinction among the Rhynchonelliformea, especially the clades that produced a laminar shell layer, the Strophomenata, and the selective survival of species secreting a shell consisting of fibres, the Rhynchonellata (Garbelli et al. 2017).

The emergence of thecideides is not strictly related to the End-Permian extinction as they appeared about 20 million years after this event (e.g. Baker 2006). However, as benthic palaeocommunities were increasingly dominated by bivalves during the Triassic and Jurassic and, as free-living and pedicle-attached rhynchonellide and terebratulide brachiopods became less common (e.g. Clapham & Bottjer 2007; Liow et al. 2015), the emerging thecideides developed shell cementation to the substrate. Thecideides are found today and in the fossil record in cryptic habitats, caves or/and surfaces below rock overhangs and are associated, in contrast to most other fossil and extant rhynchonelliform brachiopods, cemented to hard substrates. Their growth is confined to small body sizes. It might well be that fibrous microstructures are less suitable for a cemented lifestyle; thus, accordingly, shell microstructure, the mineral units, their assembly and degree of co-orientation had to change. The change in lifestyle and hard tissue microstructure might have initiated the small shell

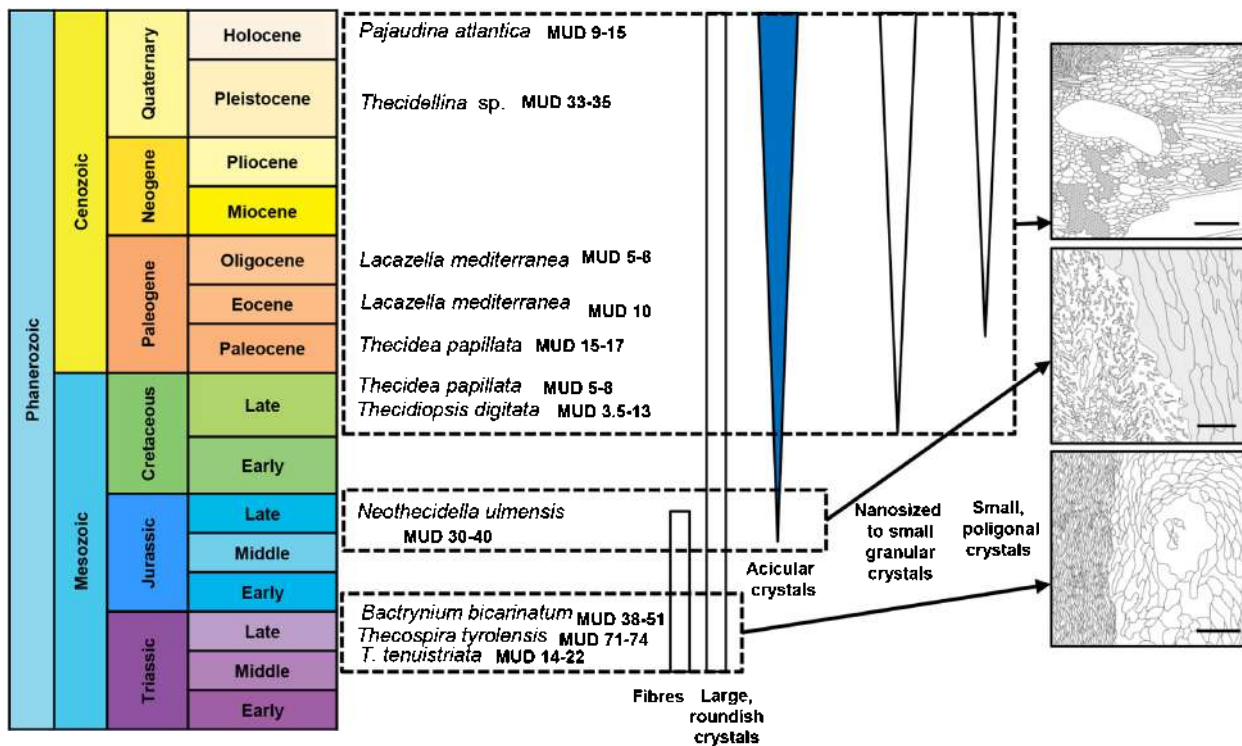


Fig. 14. Summary of the investigated suite of thecideide brachiopods, their stratigraphical distribution and schematic illustrations of the main microstructure characteristics of their shells. See scale bar values in Figure 12. [Colour figure can be viewed at wileyonlinelibrary.com]

size of modern thecideides. It is well established that the composite nature and hierarchical component organization of structural biomaterials allows for the development of many hard tissue design concepts (e.g. Mayer 2005; Fratzi & Weinkamer 2007; Dunlop & Fratzi 2010). Accordingly, Recent carbonate biological structural materials exhibit a vast diversity of microstructure and texture patterns (e.g. Huber *et al.* 2015; Griesshaber *et al.* 2017; Casella *et al.* 2018; Checa 2018; Checa *et al.* 2018; Seidl *et al.* 2018; Checa *et al.* 2019), where both, almost unaligned and highly co-aligned crystal assemblies, are utilized, if necessary. Thus, both a high order and a high disorder in biomineral unit arrangement and crystallite orientation are advantageous in certain circumstances for the organism. Microstructure and texture patterns influence directly mechanical properties of structural materials. Different environments, for example high energy settings in shallow waters or substrates in quieter, deeper waters with higher water loads, require shells with different amounts of hardness, stiffness, toughness, tensile strengths and ductility. These characteristics are imparted by the mineral-biopolymer arrangement within the hard tissue and reflect directly conditions that are defined by a given habitat (Seidl *et al.* 2012; Huber *et al.* 2015; Griesshaber *et al.* 2017; Seidl *et al.* 2018; Ye *et al.* 2018a, 2018b).

Accordingly, we infer that the evolution of thecideide shell microstructures and textures, the change from fibres to acicles, the switch from large mineral units to small and granular biominerals, the transition from an ordered to a highly disordered microstructure and texture reflect their success in colonizing hard substrates by cementation and the occupation of niches not yet capitalised by bivalves or/and rhynchonellide and terebratulide brachiopods. Several observations support these hypotheses: (1) taxa that had a similar life strategy in the Palaeozoic, cementation to hard substrates (e.g. some taxa of the Class Strophomenata), had a laminar and not a fibrous fabric (McGhee 1999; Williams *et al.* 2000; Ye *et al.* in press). Fibrous assemblies appear to be less suitable for a cemented lifestyle; (2) the Craniiformea also lived and live cemented to hard substrates and form shells with a distinct organocarbonate tabular laminar fabric (Williams 1997); (3) the granular–acicular fabric can possibly be secreted more easily and rapidly relative to the formation of fibres and columns; and (4) secretion of small mineral units, acicles and granules, might make it easier to attach to uneven substrate surfaces.

We can support the last suggestion based on the study of the microstructure of other shell-attached benthic organisms such as the Recent oyster

*Magallana gigas* (formerly *Crassostrea gigas* (Thunberg 1793)) which lives cemented to many types of substrates (MacDonald *et al.* 2010). Our EBSD measurements show that for attachment, *M. gigas* secretes a shell layer of variable thickness that consists of minute to small, irregularly sized, shaped and oriented calcite crystals (Figs S17, S18). Crystal co-orientation within the layer that attaches to the substrate is low; it is significantly less than the co-orientation of calcite in the adjacent foliated shell layers (Fig. S17). The many different orientations and the small size of those crystallites that touch the surface of the substrate make it easier for the oyster to adjust to the roughness of the surface.

Rudwick (1968) and Pajaud (1974) showed that the attachment scar on the ventral valve in some Triassic and Cretaceous thecideides became obsolete in larger specimens (as the ventral valve increased in convexity and the dorsal valve in concavity) and suggested that such individuals were secondarily free-lying in adult stages. In contrast, Recent thecideides are permanently cemented to substrates. The gradual shift from fibrous to acicular structures seems to coincide with an overall shift in the living strategy of thecideides towards permanent attachment. For example, the Upper Triassic *B. bicarinatum*, also investigated in this study, is very common in offshore mudstones of the Eiberg Member of the Kössen Formation (Northern Calcareous Alps, Austria) where a free-lying life habit can be expected (see also Michalik 1976).

In transitional forms (e.g. *N. ulmensis*), the fibrous layer is partly replaced by stacks of acicles. Acicles always form outer shell portions, while the arrays of fibres are always next to the soft tissue of the animal. The progressive loss of fibres in favour of a more disordered acicular and granular microstructures is a loss which is a derived feature according to Baker (2006). This can be considered as part of the complex mosaic of pedomorphic and peramorphic patterns of evolutionary changes observed for the thecideides (Carlson 2016).

## Conclusions

EBSD measurements have demonstrated the large variety of mineral units that form thecideide shells from Late Triassic to Recent. These range from fibres through acicles to granules which are irregularly shaped and sized calcite biocrystals. Thecideide biomineral units and their arrangements differ significantly from those of terebratulide and rhynchonellide species. Based on our analyses, we draw the following conclusions:



- The regularity of biocrystal shape, mineral unit size and the degree of calcite co-orientation decreases from the Late Triassic to Recent species.
- The shell of Late Jurassic species represent transitional forms and are composed of stacks of acicles on external shell portions and of a remnant of the fibrous layer next to the soft tissue of the animal.
- The change in microstructure and texture may be interpreted as an ecological strategy to exploit distinct habitats and lifestyles, in particular attachment to hard substrates, as confirmed by a microstructural comparison with recent bivalves that live attached to rock substrates.
- The progressive loss of the fibrous layer in favour of highly disordered acicular and granular microstructures can be seen as a paedomorphic pattern in the complex mosaic of evolutionary changes characterizing thecideid brachiopods.
- Detailed shell microstructure and texture data gained from EBSD measurements are needed from more thecideid taxa in order to unravel their phylogenetic relationships.

*Acknowledgements.* – This project has received funding from the European Union's Horizon 2020 research and innovation programme under grant agreement no 643084. We thank Prof. Dr A. Checa (Department of Stratigraphy and Paleontology, University of Granada, Spain) for the *Magallana gigas* sample. D.A.T. Harper thanks Martin Smith (Department of Earth Sciences, Durham University, UK) for his help implementing the TreeSearch algorithm. The authors have no conflict of interest. We would like to thank the two anonymous reviewers for their constructive comments, which improved the text. Open Access funding enabled and organized by ProjektDEAL.

### Data availability statement

Additional data, that support the findings of this study, are available from the Supporting Information of this article and from the corresponding author upon reasonable request.

### References

- Backhaus, E. 1959: Monographie der cretacischen Thecideidae (Brach). *Mitteilungen aus dem Geologischen Staatsinstitut in Hamburg* 28, 5–90.
- Baker, P.G. 1990: The classification, origin and phylogeny of the thecideid brachiopods. *Palaeontology* 33, 175–191.
- Baker, P.G. 2006: Thecideida. In Kaesler, R.L. (ed.): *Treatise on Invertebrate Paleontology Part H. Brachiopoda 5 (revised)*, 1938–1943. Geological Society of America, Boulder, and University of Kansas Press, Lawrence.
- Baker, P.G. & Laurie, K. 1978: Revision of Aptian thecideid brachiopods of the Faringdon Sponge Gravels. *Palaeontology* 21, 555–570.
- Baker, P.G. & Logan, A. 2011: Support from early juvenile Jurassic, Cretaceous and Holocene thecideid species for a postulated common early ontogenetic development pattern in thecideid brachiopods. *Palaeontology* 54, 111–131.
- Baumgarten, S., Laudien, J., Jantzen, C. & Häussermann, V. 2013: Population structure, growth and production of a modern brachiopod from the Chilen fjord region. *Marine Ecology* 35, 401–413.
- Bittner, A. 1890: Brachiopoden der Alpenen Trias. *Abhandlungen der Kaiserlich-Königlichen Geologischen Reichsanstalt* 14, 1–325.
- Brazeau, M.D., Guillerme, T. & Smith, M.R. 2019: An algorithm for morphological phylogenetic analyses with inapplicable data. *Systematic Biology* 68, 619–631.
- Carlson, S.J. 1995: Phylogenetic relationships among extant brachiopods. *Cladistics* 11, 131–197.
- Carlson, S.J. 2007: Recent research on brachiopod evolution. 2878–2900. In Selden, P.A. (ed): *Treatise on Invertebrate Paleontology, Part H, Brachiopoda (revised)*, volume 6, 956. Geological Society of America, Boulder and University of Kansas Press, Lawrence.
- Carlson, S.J. 2016: The evolution of Brachiopoda. *Annual Review of Earth and Planetary Sciences* 44, 409–438.
- Casella, L.A., Griesshaber, E., Simonet-Roda, M., Ziegler, A., Mavromatis, V., Henkel, D., Laudien, J., Häussermann, V., Neuser, R.D., Angiolini, L., Dietzel, M., Eisenhauer, A., Immenhauser, A., Brand, U. & Schmahl, W.W. 2018: Micro- and nanostructures reflect the degree of diagenetic alteration in modern and fossil brachiopod shell calcite: a multi-analytical screening approach (CL, FE-SEM, AFM, EBSD). *Palaeogeography, Palaeoclimatology, Palaeoecology* 502, 13–30.
- Checa, A. 2018: Physical and biological determinants of the fabrication of molluscan shell microstructures. *Frontiers in Marine Science* 5, 353.
- Checa, A., Harper, E. & Gonzalez Segura, A. 2018: Structure and crystallography of foliated and chalk shell microstructures of the oyster *Magallana*: the same materials grown under different conditions. *Scientific Reports* 8, 7507.
- Checa, A., Salas, C., Rodriguez-Navarro, A., Grenier, C. & Lagos, N. 2019: Articulation and growth of skeletal elements in balanid barnacles (Balanidae, Balanomorpha, Cirripedia). *Royal Society Open Science* 6, 190458.
- Clapham, M.E. & Bottjer, D.J. 2007: Prolonged Permian Triassic ecological crisis recorded by molluscan dominance in the Late Permian offshore assemblages. *Proceedings of the National Academy of Sciences of the United States of America* 104, 12971–12975.
- Cohen, B.L. 2007: The brachiopod genome. In Selden, P.A. (ed.): *Treatise on Invertebrate Paleontology. Part H (supplement), Brachiopoda (revised)*, volume 6, 2356–2372. Geological Society of America, Boulder, and University of Kansas Press, Lawrence, 956 pp.
- Crippa, G., Ye, F., Malinverno, C. & Rizzi, A. 2016: Which is the best method to prepare invertebrate shells for SEM analysis? Testing different techniques on recent and fossil brachiopods. *Bollettino della Societa Paleontologica* 55, 111–125.
- Dagys, A.S. 1972: Ultrastructure of thecospirid shells and their position in brachiopod systematics. *Paleontological Journal* 6, 359–369.
- Dunlop, J.W.C. & Fratzl, P. 2010: Biological composites. *Annual Review of Materials Research* 40, 1–24.
- Elliot, G.F. 1953: The classification of the thecidean brachiopods. *The Annals and Magazine of Natural History* 6, 693–701.
- Emmrich, H. 1855: II. Notiz über den Alpenkalk der Lienzer Gegend. *Jahrbuch der Geologischen Bundesanstalt* 6, 444–450.
- Fratzl, P. & Weinkarmer, R. 2007: Nature's hierarchical materials. *Progress in Material Science* 52, 1263–1334.
- Frisia, S. 1990: TEM investigation of the shell of the brachiopod *Thecospira tyrolensis* (Loretz): a clue to understanding growth and replacement of prismatic and/or fibrous low mg-calcite? *Rivista Italiana di Paleontologia e Stratigrafia* 96, 77–92.
- Garbelli, C., Angiolini, L., Brand, U. & Jadoul, F. 2014: Brachiopod fabric, classes and biogeochemistry: implications for the reconstruction and interpretation of seawater carbon-isotope curves and records. *Chemical Geology* 371, 60–67.

- Garbelli, C., Angiolini, L. & Shen, S.-Z. 2017: Biomineralization and global change: a new perspective for understanding the end-Permian extinction. *Geology* 45, 19–22.
- Goetz, A.J., Griesshaber, E., Neuser, R.D.L., Harper, E. & Schmahl, W.W. 2009: Calcite morphology, texture and hardness in the distinct layers of rhynchonelliform brachiopod shells. *European Journal of Mineralogy* 21, 303–315.
- Goetz, A.J., Steinmetz, D.R., Griesshaber, E., Zaefferer, S., Raabe, D., Kelm, K., Irsen, S., Sehrbrock, A. & Schmahl, W.W. 2011: Interdigitating biocalcite dendrites form a 3-D jigsaw structure in brachiopod shells. *Acta Biomaterialia* 7, 2237–2243.
- Grant, R.E. 1972: The lophophore and feeding mechanism of the Productidina (Brachiopoda). *Journal of Paleontology* 46, 213–250.
- Greiner, M., Yin, X., Fernández-Díaz, L., Griesshaber, E., Weitzel, F., Ziegler, A., Veintemillas-Verdaguer, S. & Schmahl, W.W. 2018: Combined influence of reagent concentrations and agar hydrogel strength on the formation of biomimetic hydrogel-calcite composite. *Crystal Growth and Design* 18, 1401–1414.
- Griesshaber, E., Goetz, A.J., Howard, L., Ball, A., Ruff, S. & Schmahl, W.W. 2012: Crystal architecture of the tooth and jaw bone (pyramid) of the sea urchin *Paracentrotus lividus*. *Bioinspired Biomimetic and Nanobiomaterials* 1, 133–139.
- Griesshaber, E., Kelm, K., Sehrbrock, A., Mader, W., Mutterlose, J., Brand, U. & Schmahl, W.W. 2009: Amorphous calcium carbonate in the shell material of the brachiopod *Megerlia truncata*. *European Journal of Mineralogy* 21, 715–723.
- Griesshaber, E., Schmahl, W.W., Neuser, R., Pettke, T., Blüm, M., Mutterlose, J. & Brand, U. 2007: Crystallographic texture and microstructure of terebratulide brachiopod shell calcite: an optimized materials design with hierarchical architecture. *American Mineralogist* 92, 722–734.
- Griesshaber, E., Yin, X., Ziegler, A., Kelm, K., Checa, A., Eisenhauer, A. & Schmahl, W.W. 2017: Patterns of mineral organization in carbonate biological hard materials. In Heuss-Abbichler, S., Amthauer, G. & John, M. (eds): *Highlights in Applied Mineralogy*, 245–272. De Gruyter, Berlin, Boston, 360 pp.
- He, W.-H., Shi, G.R., Zhang, K.-X., Yang, T.-L., Shen, S.-Z. & Zhang, Y. 2019: *Brachiopods around the Permian-Triassic Boundary of South China. New Records of the Great Dying in South China*, 261 pp. Gateway East, Singapore: Springer.
- Huber, J., Griesshaber, E., Nindiyasari, F., Schmahl, W.W. & Ziegler, A. 2015: Functionalization of biomineral reinforcement in crustacean cuticle: calcite orientation in the partes incisivae of the mandibles of *Porcellio scaber* and the supralittoral species *Tylos europaeus* (Oniscidea, Isopoda). *Journal of Structural Biology* 190, 173–191.
- Jaecks, G.S. & Carlson, S.J. 2001: How phylogenetic inference can shape our view of heterochrony: examples from thecideide brachiopods. *Paleobiology* 27, 205–225.
- Krawczyński, C. 2008: The Upper Oxfordian (Jurassic) thecideide brachiopods from the Kujawy area, Poland. *Acta Geologica Polonica* 58, 395–406.
- Liow, L.H., Reitan, T. & Harnik, P.G. 2015: Ecological interactions on macroevolutionary time scales: clams and brachiopods are more than ships that pass in the night. *Ecology Letters* 18, 1030–1039.
- Logan, A. 1988: A new thecideid genus and species (Brachiopoda, Recent) from the southeast North Atlantic. *Journal of Paleontology* 62, 546–551.
- Loretz, H. 1875: Einige Petrefacten der alpinen Trias aus den Südalpen. *Zeitschrift der Deutschen Geologischen Gesellschaft* 27, 784–841.
- Lüter, C. 2005: The first modern species of the unusual brachiopod *Kakanuiella* (Thecideidae) from New Zealand deep waters. *Systematics and Biodiversity* 3, 105–111.
- MacDonald, J., Freer, A. & Cusack, M. 2010: Attachment of oysters to natural substrata by biologically induced marine carbonate cement. *Marine Biology* 157, 2087–2095.
- Mackinnon, D.I. 1974: The shell structure of spiriferide Brachiopoda. *Bulletin of the British Museum of Natural History (Geology)* 25, 189–261.
- Mayer, G. 2005: Rigid biological systems as models for synthetic composites. *Science* 310, 1144–1147.
- McGhee, G.R. Jr 1999: The theoretical enigma of non-biconvex brachiopod shell form. In Savazzi, E. (ed): *Functional Morphology of the Invertebrate Skeleton*, 429–433. Wiley & Sons, Chichester, New York, 706 pp.
- Michalik, J. 1976: Two representatives of Strophomenida (Brachiopoda) in the uppermost Triassic of the West Carpathians. *Geologica Carpathica* 27, 79–96.
- Pajaud, D. 1970: Monographies des Thécidées (Brachiopodes). *Mémoires de la Société géologique de France* 112, 1–349.
- Pajaud, D. 1974: Écologie des Thécidées. *Lethaia* 7, 203–218.
- Quenstedt, F.A. 1858: *Der Jura*, 842 pp. Laupp, Tübingen.
- Risso, A. 1826: Histoire naturelle des principales productions de l'Europe méridionale, et particulièrement de celles des environs de Nice et des Alpes Maritimes. IV. *Aperçu sur l'Histoire Naturelle des mollusques et des coquilles de l'Europe Méridionale* 7, 439.
- Rudwick, M.J.S. 1968: The feeding mechanisms and affinities of the Triassic brachiopods *Thecospira* Zugmayer and *Bactrynum* Emmrich. *Palaeontology* 11, 329–360.
- Rudwick, M.J.S. 1970: *Living and fossil brachiopods*, 199 pp. Hutchinson University Library, London.
- von Schlotheim, E.F. 1813: Beiträge zur Naturgeschichte der Versteinerungen in geognostischer Hinsicht. In Leonhard, C.C. (ed): *Taschenbuch für die gesammte Mineralogie mit Hinsicht auf die neuesten Entdeckungen*, volume 7, 340. Hermannsche Buchhandlung, Frankfurt am Main.
- Schmahl, W.W., Griesshaber, E., Neuser, R., Lenze, A., Job, R. & Brand, U. 2004: The microstructure of the fibrous layer of terebratulide brachiopod shell calcite. *European Journal of Mineralogy* 16, 693–697.
- Schmahl, W.W., Griesshaber, E., Kelm, K., Goetz, A., Jordan, G., Ball, A., Xu, D., Merkel, C. & Brand, U. 2012: Hierarchical structure of marine shell biomaterials: biomechanical functionalization of calcite by brachiopods. *Zeitschrift für Kristallographie* 227, 793–804.
- Schwartz, A., Kumar, M., Adams, B. & Field, D. 2000: *Electron Backscatter Diffraction in Materials Science*, 393 pp. Springer, Boston.
- Seidl, B., Griesshaber, E., Fabritius, H.O., Reisecker, C., Hild, S., Taiti, S., Schmahl, W. & Ziegler, A. 2018: Tailored disorder in calcite organization in tergite cuticle of the supralittoral isopod *Tylos europaeus*, Arcangeli, 1938. *Journal of Structural Biology* 204, 464–480.
- Seidl, B., Reisecker, C., Hild, S., Griesshaber, E. & Ziegler, A. 2012: Calcite distribution and orientation in the tergite exocuticle of the isopods *Porcellio scaber* and *Armadillidium vulgare* (Oniscidea, Crustacea). *Zeitschrift für Kristallographie* 227, 777–792.
- Simonet Roda, M., Griesshaber, E., Ziegler, A., Rupp, U., Yin, X., Henkel, D., Häussermann, V., Laudien, J., Brand, U., Eisenhauer, A., Checa, A.G. & Schmahl, W.W. 2019b: Calcite fibre formation in modern brachiopod shells. *Scientific Reports* 9, 598.
- Simonet Roda, M., Ziegler, A., Griesshaber, E., Yin, X., Rupp, U., Greiner, M., Henkel, D., Häussermann, V., Eisenhauer, A., Laudien, J. & Schmahl, W.W. 2019a: Terebratulide brachiopod shell biomineralization by mantle epithelial cells. *Journal of Structural Biology* 207, 136–157.
- Sowerby, G.B. 1823: *The Genera of Recent and Fossil Shells, for the Use of Students in Conchology and Geology*, 578 pp. Stirling, London.
- Thunberg, C.P. 1793: Tekning och Beskrifning på en stor Ostronsort ifrån Japan. *Kongliga Vetenskaps Academiens Nya Handlingar* 14, 140–142.
- Williams, A. 1973: The secretion and structural evolution of the shell of Thecideidine brachiopods. *Philosophical Transactions of the Royal Society B* 264, 439–478.
- Williams, A. 1997: Shell structure. In Kaesler, R.L. (ed): *Treatise on Invertebrate Paleontology. Part H, Brachiopoda (revised)*, volume 1, 267–320. Geological Society of America, Boulder and University of Kansas. Lawrence, 539 pp.

- Williams, A., Brunton, C.H.C. & Cocks, L.R.M. 2000: Strophomenata. In Kaesler, R.L. (ed.): *Treatise on Invertebrate Paleontology. Part H, Brachiopoda (revised)*, volume 2, 215–708. Geological Society of America, Boulder, and University of Kansas, Lawrence, 423 pp.
- Williams, A. & Carlson, S.J. 2007: Affinities of brachiopods and trends in their evolution. In Selden, P.A. (ed.): *Treatise on invertebrate Paleontology, Part H, Brachiopoda (revised)*, volume 6, 2822–2877. Geological Society of America, Boulder and University of Kansas Press, Lawrence, 956 pp.
- Williams, A. & Cusack, M. 2007: Chemostructural diversity of the brachiopod shell. In Selden, P.A. (ed.): *Treatise on Invertebrate Paleontology, Part H, Brachiopoda (revised)*, volume 6, 2396–2521. Geological Society of America, Boulder and University of Kansas Press, Lawrence.
- Ye, F., Crippa, G., Garbelli, C. & Griesshaber, E. 2018a: Microstructural data of six modern brachiopod species: SEM, EBSD, morphometric and statistical analyses. *Data in Brief* 18, 300–318.
- Ye, F., Crippa, G., Angiolini, L., Brand, U., Capitani, G., Cusack, M., Garbelli, C., Griesshaber, E., Harper, E. & Schmahl, W. 2018b: Mapping of modern brachiopod microstructure: a tool for environmental studies. *Journal of Structural Biology* 201, 221–236.
- Ye Facheng, Garbelli Claudio, Shen Shuzhong, Angiolini Lucia (2020) The shell fabric of Palaeozoic brachiopods: patterns and trends. *Lethaia*, <https://doi.org/10.1111/let.12412>.
- Yin, X., Griesshaber, E., Fernández-Díaz, L., Ziegler, A., García-García, F. & Schmahl, W. 2019: Influence of gelatin-agarose composites and Mg on hydrogel-carbonate aggregate formation and architecture. *Crystal Growth and Design* 19, 5696–5715.

## Supporting Information

Additional supporting information may be found online in the Supporting Information section at the end of the article.

**Table S1.** Sample information and numbers for the illustrated material.

**Table S2.** The character matrix and taxa used for construction of the phylogenetic tree (see also Fig. 13), based on the characters and character states described by Jaecks & Carlson (2001) with the addition of microstructure and texture results obtained in this study and the inclusion of the thecideide species *Neothecidella ulmensis*. Character numbers referring to microstructure and texture and character states are as follows: 38, dorsal valve, extent of fibrous layer. 0 = covers entire valve; 1 = partial coverage; 2 = partial coverage, limited to sockets and/or cardinal process; 3 = absent. 39, ventral valve, extent of fibrous layer. 0 = covers entire valve; 1 = partial coverage; 2 = partial coverage, teeth only; 3 = absent. 40, dorsal valve granular calcite. 0 = absent; 1 = present. 41, Ventral valve granular calcite. 0 = absent; 1 = present. 42, dorsal valve acicular calcite. 0 = absent; 1 = present. 43, Ventral valve acicular calcite. 0 = absent; 1 = present. 50, Secondary fabric type. 0 = non-fibrous; 1 = fibrous.

**Fig. S1.** EBSD band contrast measurement image of the shell microstructure of the Triassic thecideide brachiopod *Thecospira tenuistriata* (MPU5804). The shell comprises small and large fibres and large rounded calcite units (shown by stars). Scale bars represent 100  $\mu\text{m}$ .

**Fig. S2.** BSE images of shell layers of the Jurassic thecideide brachiopod *Neothecidella ulmensis* (LMU-NU01). Two microstructures form the shell of this species: acicles and fibres. Figures (A) and (B) show the distribution of the two microstructures in the dorsal (A) and ventral (B) valve, respectively. Acicular and fibrous shell portions are clearly distinguishable, see dashed yellow line. (C) is a detailed image of the acicles, in the left upper region the acicles are less dense in comparison with the right lower region. (D), (E) and (F) are detailed images of the contact between acicular and fibrous shell layers and the interdigitation of these. Scale bar represent 250  $\mu\text{m}$  for A and B, 50  $\mu\text{m}$  for C, E and F and 20  $\mu\text{m}$  for D.

**Fig. S3.** Calcite orientation (shown colour-coded) and band contrast measurement images (shown grey-scaled) in the Jurassic thecideide brachiopod *Neothecidella ulmensis* (LMU-NU01) visualizing shell layers consisting of acicles (coloured) and of fibres (in grey), respectively. As the MUD values show, the degree of co-orientation in the fibrous shell is higher (grey-scaled), relative to acicular shell layers (coloured). Scale bars represent 20  $\mu\text{m}$ .

**Fig. S4.** A further EBSD scan made on the shell of *Neothecidella ulmensis* (LMU-NU01). Depicting calcite orientation (in colour), band contrast measurement (grey-scaled) images and pole figures and giving MUD values for the acicular and fibrous shell portions. Scale bar represents 50  $\mu\text{m}$ . The EBSD colour code is given in the figure.

**Fig. S5.** Orientation pattern of calcite shown colour-coded and derived from EBSD measurements for the shell of the Triassic thecideide brachiopod *Bactrynum bicarinatum* (E100-18-17). The EBSD colour code is given by the IPF triangle shown in Figure S4. Scale bar represents 50  $\mu\text{m}$ .

**Fig. S6.** Orientation pattern of calcite shown colour-coded and derived from EBSD measurements for the shell of the Triassic thecideide brachiopod *Thecospira tenuistriata* (MPU5784-4). The MUD value for the array of fibres is 26; 31 for fibres and the large roundish calcite crystals and 394 for an individual large roundish calcite unit. The EBSD colour code is given by the IPF triangle shown in Figure S4. Scale bars represent 50  $\mu\text{m}$ .

**Fig. S7.** Orientation pattern of calcite shown colour-coded and derived from EBSD measurements for the shell of the Triassic thecideide brachiopod *Thecospira tenuistriata* (MPU5804). The EBSD colour code is

given by the IPF triangle shown in Figure S4. Scale bars represent 100  $\mu\text{m}$ .

**Fig. S8.** Orientation pattern of calcite shown colour-coded and derived from EBSD measurements for the shell of the Jurassic thecideide brachiopod *Neothecidella ulmensis* (LMU-NU01). The EBSD colour code is given by the IPF triangle shown in Figure S4. Scale bars represent 20  $\mu\text{m}$ .

**Fig. S9.** Orientation pattern of calcite shown colour-coded and derived from EBSD measurements for the shell of the Cretaceous thecideide brachiopod *Thecid-iopsis digitata* (LMU-TD01). The EBSD colour code is given by the IPF triangle shown in Figure S4. Scale bar represents 200  $\mu\text{m}$ .

**Fig. S10.** Orientation pattern of calcite shown colour-coded and derived from EBSD measurements for the shell of the Cretaceous thecideide brachiopod *Thecidea papillata* (LMU-TPLC01). The EBSD colour code is given by the IPF triangle shown in Figure S4. Scale bar represents 100  $\mu\text{m}$ .

**Fig. S11.** Orientation pattern of calcite shown colour-coded and derived from EBSD measurements for the shell of the Palaeocene thecideide brachiopod *Thecidea papillata* (LMU-TPP01). The EBSD colour code is given by the IPF triangle shown in Figure S4. Scale bar represents 100  $\mu\text{m}$ .

**Fig. S12.** Orientation pattern of calcite shown colour-coded and derived from EBSD measurements for the shell of the Eocene and Oligocene thecideide brachiopod *Lacazella mediterranea* (LMU-LME01 and LMU-LMO01 respectively). The EBSD colour code is given by the IPF triangle shown in Figure S4. Scale bars represent 50  $\mu\text{m}$  for the Eocene sample and 100  $\mu\text{m}$  for Oligocene one.

**Fig. S13.** Orientation pattern of calcite shown colour-coded and derived from EBSD measurements for the shell of the Pleistocene thecideide brachiopod *Thecidellina* sp. (UF 325201). The EBSD colour code

is given by the IPF triangle shown in Figure S4. Scale bar represents 100  $\mu\text{m}$ .

**Fig. S14.** Orientation pattern of calcite shown colour-coded and derived from EBSD measurements for the shell of the Recent thecideide brachiopod *Pajaudina atlantica* (LMU-PA008). The EBSD colour code is given by the IPF triangle shown in Figure S4. Scale bar represents 20  $\mu\text{m}$ .

**Fig. S15.** Orientation pattern of calcite shown colour-coded and derived from EBSD measurements for the shell of the Recent thecideide brachiopod *Pajaudina atlantica* (LMU-PA010). The EBSD colour code is given by the IPF triangle shown in Figure S4. Scale bar represents 20  $\mu\text{m}$ .

**Fig. S16.** Orientation pattern of calcite shown colour-coded and derived from EBSD measurements for the shell of the Recent thecideide brachiopod *Pajaudina atlantica* (LMU-PA009). The EBSD colour code is given by the IPF triangle shown in Figure S4. Scale bar represents 50  $\mu\text{m}$ .

**Fig. S17.** BSE images depicting the attachment of the shell of the oyster *Magallana gigas* onto the substrate. Attachment is made by a thin mineralized layer (indicated by a star in all images) secreted by the animal. The thickness of the attachment layer varies, depending on the roughness of the substrate. Scale bars represent 10  $\mu\text{m}$  for A, B and 50  $\mu\text{m}$  for C–E.

**Fig. S18.** Orientation pattern of calcite shown with colour-coded EBSD maps and density distributions of associated pole figures for the attachment layer (A, C) and foliated calcite (B, D) of *Magallana gigas* shell. There is a significant difference in microstructure and texture: The degree of calcite co-orientation is low (MUD values 19, 21) within the attachment layer, while it is significantly higher (MUD values 38, 44) in the foliated calcite shell portion. Scale bars represent 10  $\mu\text{m}$  for A, B and 20  $\mu\text{m}$  for C, D.